

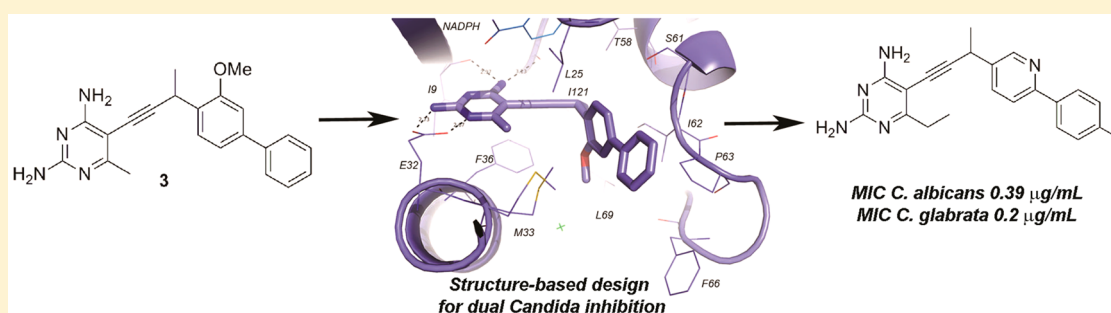
Propargyl-Linked Antifolates are Dual Inhibitors of *Candida albicans* and *Candida glabrata*

Narendran G-Dayanandan,^{†,§} Janet L. Paulsen,^{†,§} Kishore Viswanathan,[†] Santosh Keshipeddy,[†] Michael N. Lombardo,[†] Wangda Zhou,[†] Kristen M. Lamb,[†] Adrienne E. Sochia,[‡] Jeremy B. Alverson,[‡] Nigel D. Priestley,[‡] Dennis L. Wright,^{*,†} and Amy C. Anderson^{*,†}

[†]Department of Pharmaceutical Sciences, University of Connecticut, 69 N. Eagleville Road, Storrs, Connecticut 06269, United States

[‡]Department of Chemistry, University of Montana, Missoula, Montana 59812, United States

S Supporting Information



ABSTRACT: Species of *Candida*, primarily *C. albicans* and with increasing prevalence, *C. glabrata*, are responsible for the majority of fungal bloodstream infections that cause morbidity, especially among immune compromised patients. While the development of new antifungal agents that target the essential enzyme, dihydrofolate reductase (DHFR), in both *Candida* species would be ideal, previous attempts have resulted in antifolates that exhibit inconsistencies between enzyme inhibition and antifungal properties. In this article, we describe the evaluation of pairs of propargyl-linked antifolates that possess similar physicochemical properties but different shapes. All of these compounds are effective at inhibiting the fungal enzymes and the growth of *C. glabrata*; however, the inhibition of the growth of *C. albicans* is shape-dependent with extended para-linked compounds proving more effective than compact, meta-linked compounds. Using crystal structures of DHFR from *C. albicans* and *C. glabrata* bound to lead compounds, 13 new para-linked compounds designed to inhibit both species were synthesized. Eight of these compounds potentially inhibit the growth of both fungal species with three compounds displaying dual MIC values less than 1 $\mu\text{g/mL}$. Analysis of the active compounds shows that shape and distribution of polar functionality is critical in achieving dual antifungal activity.

INTRODUCTION

Although bloodstream infections (BSI) are frequently attributed to bacterial pathogens, fungal infections caused by *Candida* species actually represent the fourth leading cause of BSI in the United States and present a specific risk for immune compromised patients.^{1–3} The incidence of candidiasis has increased dramatically over the previous two decades,^{2,4,5} resulting in significant morbidity, mortality (40–49%),⁶ and increased healthcare costs.² Among the *Candida* spp., *C. albicans* is the primary cause of BSI (45.6%), followed by *C. glabrata* (26.0%).⁷ However, *C. glabrata* represents an increasing threat as studies show that while *C. glabrata* accounted for 18% of BSI candidemia between 1992 and 2001, that fraction rose to 26% in the time period 2001–2007.

The administration of effective empirical therapy for fungal BSI significantly reduces mortality (27% vs 46%).⁶ Unfortunately, however, there is often a significant delay in the correct diagnosis of candidiasis,^{2,6} identification of the species, and start

of therapy to which the strain is sensitive. While *C. albicans* remains relatively sensitive to azoles, flucytosine, and echinocandins, *C. glabrata* exhibits decreased sensitivity for fluconazole, with evidence of cross-resistance to other azoles such as voriconazole;^{8,9} 11% of fluconazole-resistant strains are now also resistant to echinocandins.¹⁰ The increased incidence of *C. glabrata* as a causative agent of candidiasis along with the increasing drug resistance in this strain makes new antifungals that target *C. glabrata* a clear priority. However, an ideal agent would target both *C. albicans* and *C. glabrata* as *C. albicans* infections continue to be a major health risk and the two are difficult to distinguish in a clinical setting.

Targeting the essential enzyme dihydrofolate reductase (DHFR) has proven to be an effective strategy for both prokaryotic (e.g., trimethoprim) and protozoal (e.g., pyrimeth-

Received: December 13, 2013

Published: February 25, 2014

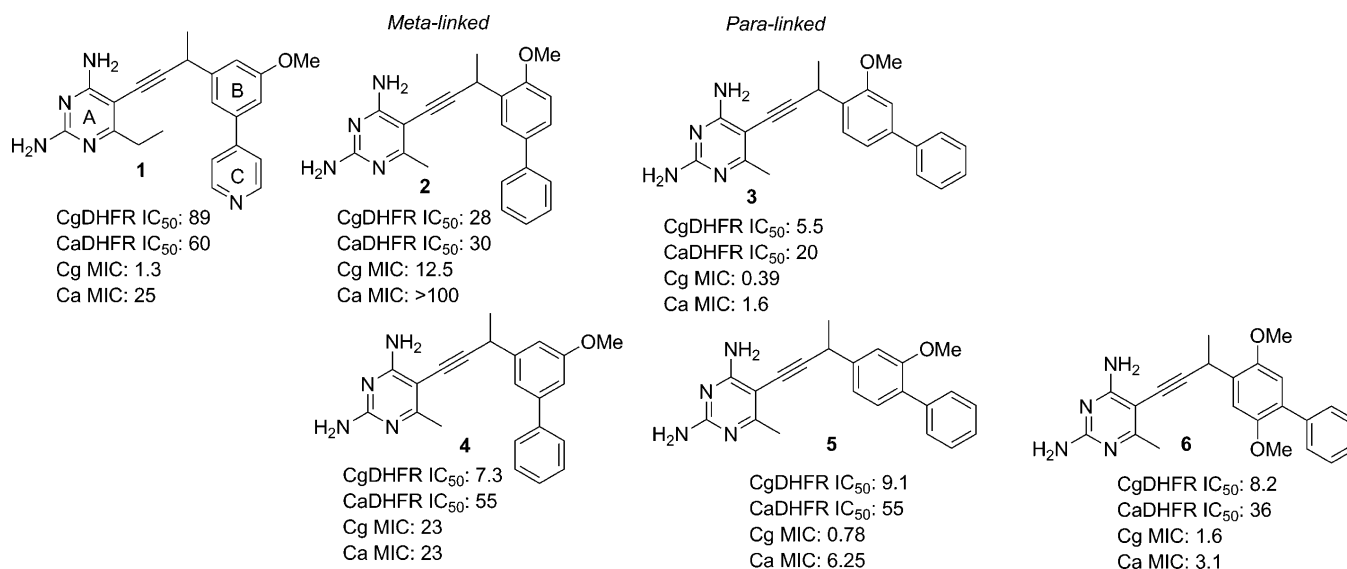


Figure 1. Shape of the propargyl-linked antifolates affects the antifungal activity. Enzyme inhibition is shown per species as an abbreviation (e.g., CgDHFR IC₅₀) with 50% inhibition concentrations (IC₅₀ values) reported in nM; MIC values are reported in μg/mL. The positional isomers for rings B and C are shown in the center of the figure.

amine) pathogens but is not widely used clinically in the treatment of invasive fungal infections. DHFR plays a critical role in the turnover of folate cofactors; effective inhibition of DHFR produces a blockade in thymidine synthesis leading to “thymineless” death. As humans are also dependent on active DHFR, it is important that there is selective inhibition of the pathogenic enzyme. Fortunately, there are several important active site differences between human and *Candida* species that can be exploited for selectivity.

It is widely recognized that the development of antimetabolites targeting *C. albicans* can be complicated by pronounced inconsistencies between target inhibition and antifungal activity.^{11–13} Attempts to study whether the cell wall or membrane permeability affects the uptake of six unrelated antibiotics targeting intracellular proteins failed to derive a direct relationship.¹³ These same inconsistencies have also complicated the development of antifungal antifolates. For example, Glaxo researchers hypothesized that molecular weight was inversely related to antifungal activity and pursued the synthesis and evaluation of over 150 low molecular weight analogues. Although the Glaxo effort produced potent, albeit nonselective inhibitors with good antifungal activity, lead optimization of the antifolates against *C. albicans* was hindered by a lack of correlation between enzyme inhibition and antifungal activity. The researchers concluded that there was no relationship between activity and inhibitor size or lipophilicity but that differences in transport phenomenon could still play an important role in antifungal activity.¹¹ More recently, a German company¹² reported a group of potent *C. albicans* DHFR inhibitors based on a benzyl(oxy)pyrimidine scaffold. However, these compounds did not exhibit *in vitro* antifungal activity. After showing that the compounds were not generally susceptible to efflux, the authors of this study also speculated that the compounds were unable to enter *C. albicans*. While these studies were conducted with *C. albicans*, it is unclear whether the same phenomenon would be observed with *C. glabrata*.

Previously, we reported a new class of antifolates possessing a 2,4-diaminopyrimidine ring linked through a propargyl bridge

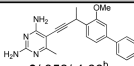
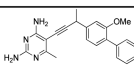
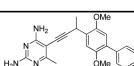
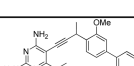
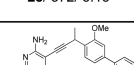
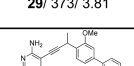
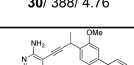
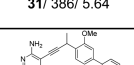
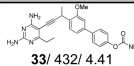
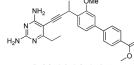
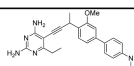
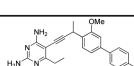
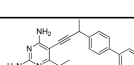
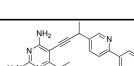
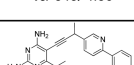
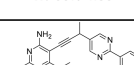
to a meta-linked biphenyl^{14,15} or biaryl¹⁶ system (example compounds 1, 2, and 4 in Figure 1) that show potent and selective inhibition of DHFR from *C. albicans* and *C. glabrata*. However, while potent inhibition of the growth of *C. glabrata* was observed with these antifolates, enzyme inhibition did not translate to antifungal activity against *C. albicans*, in a manner similar to that in previously reported studies.

As results in the literature show that target potency did not exclusively drive antifungal activity, we re-examined previously abandoned leads in the propargyl-linked antifolate series to search for potentially active chemotypes against *C. albicans*. In doing so, we identified three para-linked compounds (compounds 3, 5, and 6) that inhibit both *Candida* species. Building on this promising discovery, herein we report the synthesis and evaluation of 13 additional para-linked inhibitors and show that eight of these compounds inhibit the growth of both *Candida* species, with three showing very potent antifungal activity (MIC values of <1 μg/mL). Analysis of crystal structures of DHFR from both species bound to para-linked antifolates correlates with structure–activity relationships to reveal that hydrophobic functionality at the C-ring improves the potency of enzyme inhibition. These development studies represent a significant advance toward achieving a propargyl-linked antifolate as a single agent that potently targets both major species of *Candida*. Furthermore, preliminary studies reported here suggest that in addition to inhibitor potency at the enzyme level, there is a second critical relationship between the shape of the inhibitor, dictated here by the positional isomers of the ring systems, and antifungal activity. These compounds may also be useful to permit comparative studies between the two *Candida* species.

RESULTS

The meta-heterobiaryl propargyl-linked antifolates (such as compound 1 in Figure 1) are potent inhibitors of DHFR from both *C. glabrata* and *C. albicans*, with many compounds having 50% inhibition concentrations (IC₅₀) under 100 nM¹⁶ and a large number of interactions with active site residues (Supporting Information, Figure S1). However, despite the

Table 1. Biological Evaluation of Propargyl-Linked Antifolates

Compound	IC ₅₀ CgDHFR (nM) (selectivity ^a)	IC ₅₀ CaDHFR (nM) (selectivity)	IC ₅₀ hDHFR (nM)	MIC <i>C.</i> <i>glabrata</i> (μg/mL)	MIC <i>C.</i> <i>albicans</i> (μg/mL)	IC ₅₀ human MCF-10 (μM)
 3 / 358/ 4.66 ^b	5.5 (62)	20 (17)	340	0.39	1.6	74
 5 / 358/ 4.66	9.1 (156)	55 (26)	1420	0.78	6.25	80
 6 / 388/ 4.54	8.2 (38)	36 (9)	314	1.6	3.1	63
 28 / 372/ 5.15	31 (6)	49 (4)	172	1.6	6.3	ND ^c
 29 / 373/ 3.81	19 (7)	33 (4)	127	0.78	25	216
 30 / 388/ 4.76	15 (9)	39 (3)	136	3.1	NA ^d	148
 31 / 386/ 5.64	22 (9)	48 (4)	208	1.6	3.1	ND
 32 / 397/	18 (26)	50 (10)	477	7.5	3.1	50
 33 / 432/ 4.41	8 (21)	18 (9)	170	6.3	NA	ND
 34 / 431/ 4.97	9 (5)	46 (1)	49	7.5	6.25	96
 35 / 416/ 5.43	15 (10)	64 (2)	147	25	NA	ND
 36 / 390/ 5.31	14 (11)	43 (3)	148	7.5	1.8	60
 37 / 342/ 5.28	6 (29)	23 (8)	174	3.1	7.5	505
 46 / 343/ 4.36	23 (30)	55 (13)	688	0.78	0.39	148
 47 / 357/ 4.85	27 (23)	49 (13)	625	0.2	0.39	80
 48 / 344/ 4.23	22 (8)	37 (5)	180	0.78	0.19	216

^aSelectivity is calculated as IC₅₀ for the fungal enzyme/IC₅₀ for the human enzyme. ^bCompound number/MW/clogP. ^cND: not determined. ^dNA: not active at 100 μg/mL.

fact that these compounds are also potent inhibitors of the growth of *C. glabrata*, these meta-linked compounds were unable to potently inhibit *C. albicans*. For example, compound **1** inhibits *C. glabrata* and *C. albicans* DHFR with IC₅₀ values of 89 and 60 nM yet inhibits *C. glabrata* and *C. albicans* with MIC values of 1.3 μg/mL and 25 μg/mL, respectively. In an attempt to determine whether permeability may explain the differential antifungal activity of the propargyl-linked antifolates, we measured MIC values for compound **1** in the presence of 0.01% Triton X-100. Triton X-100 is known to increase membrane permeability without denaturation.¹⁷ The experiments show that in the presence of Triton X-100, the MIC values for compound **1** significantly decreased (25 to 6.25 μg/mL). These results suggest that permeability may influence antifungal activity.

As our prior work had shown that compounds with different physicochemical properties or shapes displayed differential antifungal activity against *C. glabrata* (for example, compare compounds **1**–**6** in Figure 1),¹⁶ we re-examined the *C. albicans* activity of several earlier scaffold types. This investigation showed that compounds containing a para-biphenyl moiety as the hydrophobic domain (e.g., compound **3**) had promising (MIC 1.6 μg/mL) activity against *C. albicans* while maintaining activity against *C. glabrata* (MIC 0.39 μg/mL) (Figure 1). These results suggested the intriguing possibility that alteration of the molecular shape greatly influences the *C. albicans* activity without diminishing activity against *C. glabrata*. This improvement in the *C. albicans* activity was then shown to extend to two other compounds in the para-biphenyl series (e.g., **5** and **6**). Also encouraging, the compounds remained selective for the fungal cells over human cells. For example, compounds **3** and **5**

inhibit the growth of MCF-10 cells at 74 and 80 μM, respectively (Table 1). These results prompted the exploration of this para-linked shape with a goal of identifying compounds that maintain enzyme inhibition and have superior antifungal activity against both *Candida* species.

Crystal Structures of Candida DHFR Bound to para-Linked Antifolates. In order to elucidate the structural basis of the affinity of the para-linked compounds for *C. glabrata* and *C. albicans* DHFR and to design more potent analogues in this series, we determined the ternary structures of the two enzymes bound to NADPH and compound **3** as well as the complex of *C. albicans* DHFR bound to NADPH and **6**. The structures were determined by molecular replacement using diffraction amplitudes extending to 1.76 Å (CaDHFR/NADPH/**3** and CaDHFR/NADPH/**6**) or 2.0 Å (CgDHFR/NADPH/**3**) (Supporting Information, Table S1). All structures contain two molecules in the asymmetric unit. Despite the fact that the crystallization conditions included a racemic mixture of the ligand, the *R*-enantiomer is the only one observed in the electron density. Interestingly, one of the two inhibitor molecules of CgDHFR/NADPH/**3** adopts a different conformation from the other inhibitor in the same asymmetric unit. One conformation points the 3'-methoxy down into the pocket enclosed by Phe 36, Leu 69, and Met 33 (Figure 2a), and the other points the methoxy toward Ser 61 to form a water-mediated hydrogen bond (Figure 2b). Similarly, one of the two molecules of CaDHFR/NADPH/**3** in the asymmetric unit exhibits the “down” conformation of the methoxy toward Phe 36 and Leu 69 at 100% occupancy (Figure 2c); the other inhibitor molecule has two conformations of the methoxy group with split 75%/25% occupancy. The “up” conformation

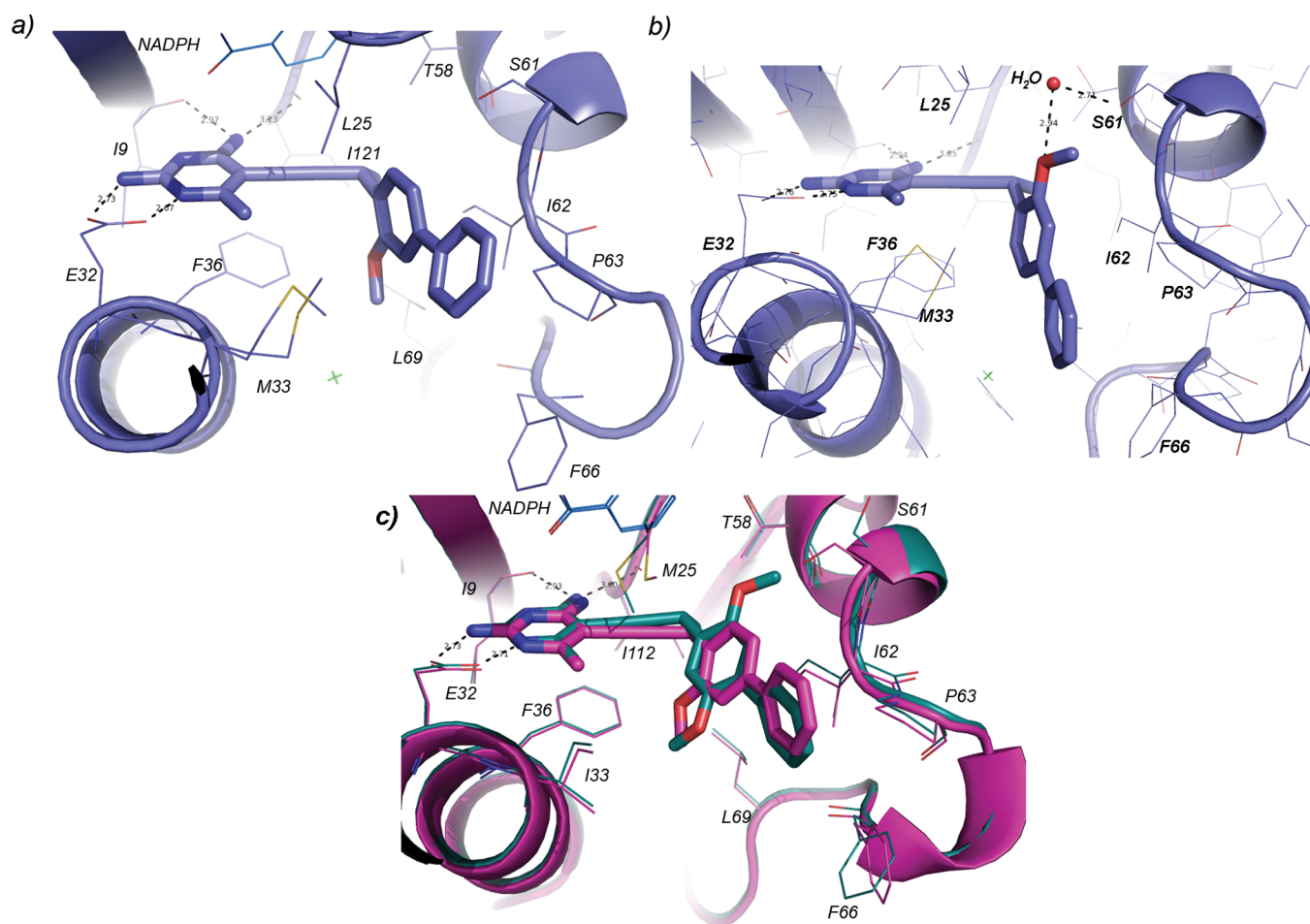
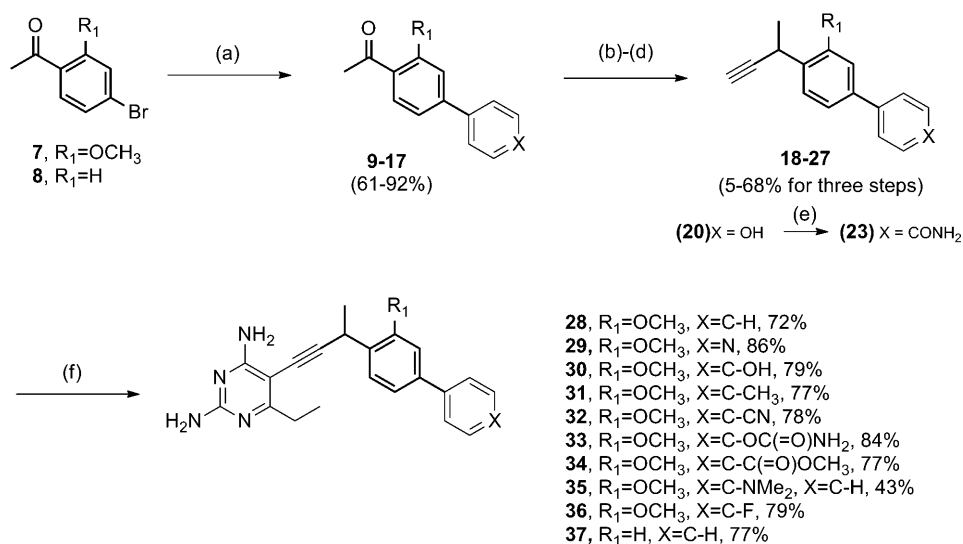


Figure 2. Crystal structures of (a) *C. glabrata* DHFR bound to NADPH and **3** (PDB ID: 4HOG) showing one conformation of the inhibitor and (b) a second conformation of the inhibitor; (c) *C. albicans* DHFR bound to **3** (PDB ID: 4HOF, magenta) and **6** (PDB ID: 4HOE, teal). Compound **3** in PDB ID 4HOF also shows two conformations of the inhibitor in chain A that are similar to those observed in the structure with *C. glabrata* DHFR.

Scheme 1^a



^a(a) Aryl-boronic acid, $\text{Pd}(\text{PPh}_3)_2\text{Cl}_2$, Cs_2CO_3 , dioxane, 80°C ; (b) $\text{Ph}_3\text{P}=\text{CHOMe}$, THF; (c) $\text{Hg}(\text{OAc})_2$, KI, THF/ H_2O ; (d) dimethyl(1-diazo-2-oxopropyl)phosphonate, K_2CO_3 , MeOH; (e) ClSO_2NCO , CH_2Cl_2 ; (f) 6-ethyl-5-iodo-2,4-diaminopyrimidine, $\text{Pd}(\text{PPh}_3)_2\text{Cl}_2$, CuI, Et_3N , DMF.

(75% occupancy) forms a water-mediated hydrogen bond between the methoxy group and Ser 61; the “down”

conformation (25% occupancy) interacts with Phe 36 and Leu 69. Overall, the inhibitors form the conserved set of

hydrogen bonds and hydrophobic interactions between the pyrimidine ring and Glu 32, Ile 9, Phe 36, Met/Ile 33, and Ile 121. The propargyl linker forms van der Waals interactions with Ile 121 and Leu 25 as well as NADPH. The biphenyl moiety forms important hydrophobic contacts with Ile 62, Pro 63, and Phe 66. The para position of the distal C-ring appeared to offer an ideal location for the introduction of functionality that could alter the physicochemical properties of the molecule without being deleterious to enzyme inhibition.

Chemistry. The dual inhibition of *C. glabrata* and *C. albicans* encouraged us to design and synthesize 10 new biphenyl inhibitors in the para-linked series of compounds with varying substitutions at the 4' position of the distal phenyl ring designed to probe the dependence of antifungal activity on physicochemical properties or to increase polarity. The synthesis of the compounds follows from previously developed routes and in brief involves the use of a central 4-bromoacetophenone moiety such as compounds 7 and 8 (Scheme 1). Suzuki cross-coupling with various aryl boronic acids gives a diverse group of biaryl derivatives (9–17) with a key acetyl group that can be taken on to the propargylated intermediates (18–27) through a three-step process. Final cross-coupling with 6-ethyl-5-iodo-2,4-diaminopyrimidine yields the panel of inhibitors (28–37).

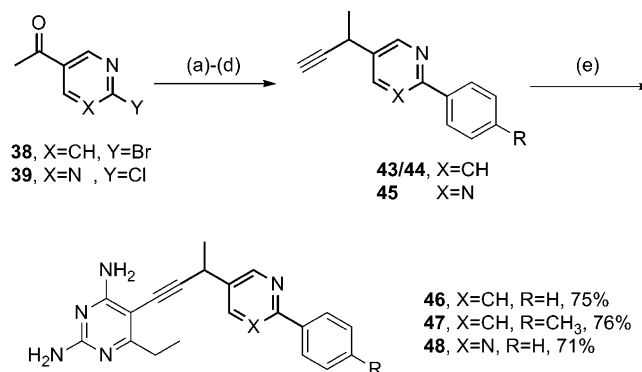
Biological Evaluation. Evaluation of a series of nine biphenyls with variable substitution on the C-ring (compounds 28 and 30–37) clearly indicates that diverse substitution at this position is well-tolerated as all compounds maintained good enzyme inhibitory activity against both species (IC_{50} values are 6–31 nM for CgDHFR and 18–64 nM for CaDHFR). However, only those compounds substituted with hydrophobic functionality at the 4-position of the distal C-ring (28, 31, 32, 36, and 37) possess significant antifungal activity against *C. albicans* with MIC values ranging from 1.8–7.5 $\mu\text{g/mL}$. These results suggest that not only the shape (para-linked C-ring) but also the para-substitution on the C-ring affects *C. albicans* activity. As we had previously observed, the activity of compound 29 against *C. glabrata* improved slightly (1.6 to 0.78 $\mu\text{g/mL}$); however, this was accompanied by a significant diminution in activity for *C. albicans* (6.3 to 25 $\mu\text{g/mL}$).

There appear to be two clusters of activities. In one cluster, compounds 35, 29, 30, and 33 with polar substituents NMe_2 , endo-N, OH, and CO_2NH_2 exhibit a significant decrease in activity. This decrease is particularly large for *C. albicans* but is also apparent for *C. glabrata*, with the noted exception of compound 29. Additionally, the compounds with polar substitutions showed decreased selectivity at the enzyme level, most likely because of interactions with the human residue, Asn 64 (Phe in both fungal species). In a second cluster, compounds 28, 37, 31, 32, and 36 with hydrophobic or electron-withdrawing substituents H, CH_3 , CN, and F maintain or show improvement in activity with noted variation between the two species.

While the SAR clearly indicated that hydrophobic functionality was preferred for activity against both species, these compounds are only moderately soluble. For example, compound 3 is soluble in water in the presence of 0.02% hydroxypropyl methylcellulose (HPMC) at 25 $\mu\text{g/mL}$. Knowing that the shape of the molecule and the position of polar functionality is a more important determinant of activity than overall molecular properties, we investigated the option of adding solubility-enhancing basic nitrogen to the proximal aromatic B-ring. Interestingly, the comparison of the activity of

compounds 28 and 37 shows that the polar 2'-methoxy is well-tolerated in this region but is not required for potency. Three new derivatives (46–48) were prepared from available pyridyl or pyrimidyl building blocks (38 and 39) using an analogous series of transformations as previously described (Scheme 2).

Scheme 2^a



^a(a) Aryl-boronic acid, $\text{Pd}(\text{PPh}_3)_2\text{Cl}_2$, Na_2CO_3 , CH_3CN , H_2O , 80°C ; (b) $\text{Ph}_3\text{P}=\text{CHOMe}$, THF; (c) $\text{Hg}(\text{OAc})_2$, KI, THF/ H_2O ; (d) dimethyl(1-diazo-2-oxopropyl)phosphonate, K_2CO_3 , MeOH; (e) 6-ethyl,5-iodo-2,4-diaminopyrimidine, $\text{Pd}(\text{PPh}_3)_2\text{Cl}_2$, CuI, Et_3N , DMF.

Excitingly, compounds 46–48 display a striking improvement in antifungal activity against both species ($\text{MIC} = 0.2\text{--}0.78 \mu\text{g/mL}$). As expected with the more permeable compounds and in contrast with compound 1, the antifungal activity of compound 47 was not significantly changed in the presence of 0.01% Triton X-100. Additionally, compounds 46 and 47 are highly selective for the fungal enzymes (13–30-fold; sequence alignment in Supporting Information, Figure S2). In contrast to the distal pyridines, incorporation of pyridine in the B-ring (compounds 46 and 47) did not provide a significant increase in solubility (20 and 15 $\mu\text{g/mL}$, respectively). However, installation of the much more polar pyrimidine group (48) increased solubility to a very good level (60 $\mu\text{g/mL}$). While compound 48 exhibited a decrease in selectivity for the fungal enzymes, it maintains an excellent level of selectivity at the cellular level with an IC_{50} against mammalian cells of 216 μM . On the basis of docking models of CaDHFR and CgDHFR bound to compound 48 (Supporting Information, Figure S3) superimposed with human DHFR, it is apparent that additional hydrophobic substituents to the C-ring may enhance selectivity by increasing interactions with Phe 66 in the fungal enzymes and decreasing interactions with Asn 64 in the human enzyme.

DISCUSSION

As reported here, the shape and distribution of polar functionality in the compounds significantly impacts the *C. glabrata* and *C. albicans* antifungal activity independent of the enzyme inhibitory potency. One hypothesis for these changes in activity could relate to differences in permeability as ineffective compounds fail to reach the intracellular target. While membrane permeability is generally thought to be related to the hydrophobicity of the compounds, the isomeric pairs shown in Figure 1 (e.g., compounds 2/3 and 4/5) possess the same clogP values, suggesting the involvement of more subtle relationships between structure and permeability. Alternative explanations for the differential antifungal activity of com-

pounds **1** and **2** could include isomer-specific sequestration by extracellular components of the cell, differences in intracellular proteins that selectively degrade some of the antifolates, or differences in efflux pump activity between the two species. Preliminary experiments to increase membrane permeability show that previously ineffective compounds (such as **1** or **2**) do inhibit the growth of *C. albicans* when treated with 0.01% Triton X-100. These results suggest that the extracellular effect on the membrane is critical and decreases the likelihood of any significant role of intracellular proteins or efflux pumps. The Triton X-100 may inactivate extracellular proteins that interfere with antifolate penetration, although this would need to be in an isomer-specific manner.

An alternative hypothesis is that ineffective compounds become sequestered in the unique cell wall of *C. albicans*. The cell wall of *C. albicans* possesses more than 20 cell wall proteins covalently attached to the skeletal layer¹⁸ and are tightly packed together, thus providing the organism with a protective protein coat and also limiting permeability.^{19–21} Cell wall proteins also tend to form phosphodiester linkages via carbohydrate side chains, giving the surface a net negative charge.^{22,23} *C. glabrata* is also known to express cell wall proteins, but much less is known about the composition of these proteins in the cell wall.²⁴ One working hypothesis is that in situations where a concentration of polar functionality is symmetrically distributed, the compound may have strong, nonselective binding to the cell wall and hence poor permeability. In contrast, compounds such as **28**, **46**, **47**, and **48** are amphipathic in their distribution of polar functionality, which may limit their sequestration and increase their permeability. Interestingly, similar trends are apparent in the Glaxo work.¹¹ In that work, potent compounds were also amphipathic with hydrophobic domains attached to the diaminopyrimidine ring; potency was decreased when these domains were di- or trimethoxybenzyl groups. The differences in activity between *C. albicans* and *C. glabrata* may relate to differences in the composition of their cell walls.

Herein we describe a significant advance in the development of propargyl-linked antifolates targeting fungal pathogens. This work has identified a new generation of analogues that are highly potent inhibitors of the DHFR enzymes as well as the growth of both *C. albicans* and *C. glabrata*. We have shown that the shape and exposed polar functionality of the compounds strongly affect the antifungal activity. These compounds may be used for further development of potent antifungal antifolates.

EXPERIMENTAL PROCEDURES

The synthesis and characterization of compounds **1–6** were previously reported in refs 25–27.

The ¹H and ¹³C NMR spectra were recorded on Bruker instruments at 500 MHz. Chemical shifts are reported in ppm and are referenced to the residual CHCl₃ solvent; 7.24 and 77.23 ppm for ¹H and ¹³C, residual solvent MeOH; 4.78, 3.31, and 49.15 ppm, respectively. Melting points were recorded on a Mel-Temp 3.0 apparatus and are uncorrected. The high-resolution mass spectrometry was provided by the Notre Dame Mass Spectrometry Laboratory and University of Connecticut Mass Spectrometry Laboratory using an AccuTOF mass spectrometer and/or using a DART source. IR data were obtained using an Alpha diamond ATR probe. TLC analyses were performed on Sorbent Technologies silica gel HL TLC plates. All glassware was oven-dried and allowed to cool under an argon atmosphere. Anhydrous dichloromethane, ether, and tetrahydrofuran were used directly from Baker Cycle-Tainers. Anhydrous dimethylformamide was purchased from Acros and degassed by purging with argon. Anhydrous

triethylamine was purchased from Aldrich and degassed by purging with argon. All reagents were used directly from commercial sources unless otherwise stated. Boronic acids for Suzuki coupling were purchased from Frontier Scientific, Inc. 4'-Bromoacetophenone and 5-acetyl-2-bromopyridine were purchased from Sigma Aldrich. The starting bromo ketones **7**,²⁸ **40**,²⁹ the Ohira–Bestmann reagent,³⁰ and 2,4-diamino-6-ethyl-5-iodopyrimidine³¹ were synthesized according to literature procedures. Purity analyses were performed with reversed phase high performance liquid chromatography (RP-HPLC) performed on a Shimadzu Prominence 20 instrument fitted with a Luna 5 μ m C18(2) 100 Å column (5 μ M, 4.6 mm \times 250 mm, Phenomenex) and detected using a UV diode array at 254 nm. Two separate determinations, method A with isocratic 50% (v/v) MeCN in 50% mM potassium phosphate monobasic at pH 7.0 and method B with isocratic 80% (v/v) MeOH in 20% mM potassium phosphate monobasic at pH 7.0, were employed to determine compound purity. Compounds were diluted in HPLC grade methanol and filtered prior to analysis. Sample concentrations were 1 mg/mL, and injection volumes were 1 μ L–3 μ L. The purity of the final compounds were found to be \geq 95% except for that of compound **35**, the purity of which could not be determined exactly because of instability.

General Procedure for Suzuki Coupling. 1-(3-Methoxy-biphenyl-4-yl)-ethanone (**9**). Ketone **7** (0.52 g, 2.20 mmol), phenylboronic acid (0.55 g, 4.50 mmol), Cs₂CO₃ (2.23 g, 6.84 mmol), Pd(PPh₃)₂Cl₂ (0.16 g, 0.22 mmol, 10% Pd), and anhydrous dioxane (8 mL) were added to 50 mL of screw cap pressure vessel. The mixture was stirred, degassed by purging with argon for 15 min, sealed, and placed in an 80 °C oil bath for 5 h. The dark colored mixture was cooled, diluted with ether, and filtered through a pad of Celite and rinsed with ether. The filtrate was concentrated and the residue purified by flash column chromatography (SiO₂, 20 g, 5% EtOAc/hexanes) to afford the biphenyl ketone **9** as a white solid (0.41 g, 79%): TLC R_f = 0.5 (25% EtOAc/hexanes); mp 72.8–74.5 °C; ¹H NMR (500 MHz, CDCl₃) δ 7.83 (d, *J* = 8.0 Hz, 1H), 7.59 (d, *J* = 7.5 Hz, 2H), 7.45 (dd, *J* = 7.3 Hz, 7.3 Hz, 1H), 7.45 (dd, *J* = 7.3 Hz, 7.3 Hz, 1H), 7.38 (m, 1H), 7.20 (d, *J* = 8.0 Hz, 1H), 7.14 (s, 1H), 3.96 (s, 3H), 2.64 (s, 3H); ¹³C NMR (125 MHz, CDCl₃) δ 199.3, 159.5, 147.0, 140.3, 131.1, 129.0, 128.3, 127.3, 126.9, 119.5, 110.5, 55.7, 32.0; IR (neat cm^{–1}) 3059, 2994, 2953, 2920, 1665, 1467, 1220, 1014, 761, 694; HRMS (DART, M⁺ + H) *m/z* 227.1088 (calculated for C₁₅H₁₅O₂, 227.1072).

1-(2-Methoxy-4-pyridin-4-yl-phenyl)-ethanone (**10**). According to the general Suzuki coupling procedure, ketone **7** (0.50 g, 2.10 mmol), pyridine-4-boronic acid (0.54 g, 4.36 mmol), Cs₂CO₃ (2.15 g, 6.55 mmol), Pd(PPh₃)₂Cl₂ (0.15 g, 0.22 mmol, 10% Pd), and anhydrous dioxane (6 mL) were heated at 80 °C for 12 h (overnight). Following the general workup and flash chromatography (SiO₂, 20 g, 50% EtOAc/hexanes), biaryl ketone **10** was obtained as a pale white solid (0.45 g, 89%): TLC R_f = 0.2 (50% EtOAc/hexanes); mp 88.8–92; ¹H NMR (500 MHz, CDCl₃) δ 8.72 (d, *J* = 5.3 Hz, 2H), 7.86 (d, *J* = 7.9 Hz, 1H), 7.55–7.52 (m, 2H), 7.27 (dd, *J* = 8.0, 1.3 Hz, 1H), 7.20 (s, 1H), 4.02 (s, 3H), 2.67 (s, 3H); ¹³C NMR (125 MHz, CDCl₃) δ 199.1, 159.3, 150.2, 132.1, 132.0, 131.2, 128.5, 121.7, 119.3, 110.2, 55.7, 31.8; IR (neat cm^{–1}) 3375, 3037, 2922, 1660, 1398, 1227, 1025, 813, 537; HRMS (DART, M⁺ + H) *m/z* 374.2003 (calculated for C₂₂H₂₄N₂O, 374.1981).

1-[3-Methoxy-4'-(tetrahydro-pyran-2-yloxy)-biphenyl-4-yl]-ethanone (**11**). According to the general Suzuki coupling procedure, ketone **7** (0.49 g, 2.17 mmol), 4-(tetrahydro-2H-pyran-2-yloxy)-phenylboronic acid (0.96 g, 4.34 mmol), Cs₂CO₃ (2.12 g, 6.51 mmol), Pd(PPh₃)₂Cl₂ (0.15 g, 0.22 mmol, 10% Pd), and anhydrous dioxane (6 mL) was heated at 80 °C for 14 h (overnight). Following the general workup and flash chromatography (SiO₂, 20 g, 10% EtOAc/hexanes), biaryl ketone **11** was obtained as a pale white solid (0.430 g, 61%): TLC R_f = 0.5 (25% EtOAc/hexanes); mp 86.7–89.7 °C; ¹H NMR (500 MHz, CDCl₃) δ 7.80 (d, *J* = 8.0 Hz, 1H), 7.52 (d, *J* = 7.9 Hz, 2H), 7.30–6.97 (m, 4H), 5.46 (s, 1H), 3.95 (s, 3H), 3.92–3.87 (m, 1H), 3.62–3.59 (m, 1H), 2.62 (s, 3H), 2.05–1.97 (m, 1H), 1.87–1.86 (m, 2H), 1.72–1.65 (m, 2H), 1.60–1.58 (m, 1H); ¹³C NMR (125 MHz, CDCl₃) δ 199.2, 159.5, 157.5, 146.7, 133.5, 131.2, 128.4, 126.3,

119.1, 116.9, 110.0, 96.4, 62.1, 55.6, 32.0, 30.4, 25.3, 18.8; IR (neat cm^{-1}) 2940, 2872, 2847, 1656, 1598, 1358, 1280, 1177, 1019, 813, 518; HRMS (DART, $\text{M}^+ + \text{H}$) m/z 327.1612 (calculated for $\text{C}_{20}\text{H}_{23}\text{O}_4$, 327.1596).

1-(3-Methoxy-4'-methyl-biphenyl-4-yl)-ethanone (12). According to the general Suzuki coupling procedure, ketone **7** (0.465 g, 2.03 mmol), 4-tolylboronic acid (0.551 g, 4.06 mmol), Cs_2CO_3 (1.98 g, 6.09 mmol), $\text{Pd}(\text{PPh}_3)_2\text{Cl}_2$ (0.142 g, 0.20 mmol, 10% Pd), and anhydrous dioxane (6 mL) were heated at 80 °C for 5 h. Following the general workup and flash chromatography (SiO_2 , 20 g, 5% EtOAc/hexanes), biaryl ketone **12** was obtained as a white solid (0.375 g, 77%); TLC R_f = 0.57 (25% EtOAc/hexanes); mp 84.2–86.1 °C; ^1H NMR (500 MHz, CDCl_3) δ 7.87 (d, J = 8.0 Hz, 1H), 7.55 (d, J = 7.6 Hz, 2H), 7.31 (d, J = 7.6 Hz, 2H), 7.24 (d, J = 8.0 Hz, 1H), 7.18 (s, 1H), 4.01 (s, 3H), 2.69 (s, 3H), 2.45 (s, 3H); ^{13}C NMR (125 MHz, CDCl_3) δ 198.9, 159.4, 146.8, 138.1, 137.1, 130.9, 129.6, 126.9, 126.4, 119.1, 110.0, 55.4, 31.8, 21.1; IR (neat cm^{-1}) 3028, 2949, 2921, 1657, 1551, 1223, 1013, 808, 510; HRMS (DART, $\text{M}^+ + \text{H}$) m/z 241.1251 (calculated for $\text{C}_{16}\text{H}_{17}\text{O}_2$, 241.1229).

4'-Acetyl-3'-methoxy-biphenyl-4-carbonitrile (13). According to the general Suzuki coupling procedure, ketone **7** (0.500 g, 2.18 mmol), 4-cyanophenylboronic acid (0.640 g, 4.36 mmol), Cs_2CO_3 (2.14 g, 6.55 mmol), $\text{Pd}(\text{PPh}_3)_2\text{Cl}_2$ (0.154 g, 0.22 mmol, 10% Pd), and anhydrous dioxane (6 mL) were heated at 80 °C for 14 h (overnight). Following the general workup and flash chromatography (SiO_2 , 20 g, 10% EtOAc/hexanes), biaryl ketone **13** was obtained as a white solid (0.470 g, 86%); TLC R_f = 0.4 (25% EtOAc/hexanes); mp 125–127.2 °C; ^1H NMR (500 MHz, CDCl_3) δ 7.84 (d, J = 8.0 Hz, 1H), 7.76–7.73 (m, 2H), 7.71–7.68 (m, 2H), 7.20 (dd, J = 8.0, 1.6 Hz, 1H), 7.13 (d, J = 1.5 Hz, 1H), 4.00 (s, 3H), 2.64 (s, 3H); ^{13}C NMR (125 MHz, CDCl_3) δ 199.2, 159.5, 144.8, 144.7, 132.9, 131.5, 128.2, 128.1, 119.8, 118.8, 112.1, 110.7, 55.9, 32.0; IR (neat cm^{-1}) 3073, 3046, 2923, 2225, 1652, 1601, 1468, 1225, 1023, 812, 543; HRMS (DART, $\text{M}^+ + \text{H}$) m/z 252.1032 (calculated for $\text{C}_{16}\text{H}_{14}\text{NO}_2$, 252.1024).

4'-Acetyl-3'-methoxy-biphenyl-4-carboxylic Acid Methyl Ester (14). According to the general Suzuki coupling procedure, ketone **7** (0.506 g, 2.21 mmol), 4-(methoxycarbonyl)phenylboronic acid (0.795 g, 4.42 mmol), Cs_2CO_3 (2.16 g, 6.63 mmol), $\text{Pd}(\text{PPh}_3)_2\text{Cl}_2$ (0.155 g, 0.22 mmol, 10% Pd), and anhydrous dioxane (6 mL) were heated at 80 °C for 14 h (overnight). Following the general workup and flash chromatography (SiO_2 , 20 g, 15% EtOAc/hexanes), biaryl ketone **14** was obtained as a white solid (0.490 g, 78%); TLC R_f = 0.4 (25% EtOAc/hexanes); mp 140.4–142.6 °C; ^1H NMR (500 MHz, CDCl_3) δ 8.09 (d, J = 8.0 Hz, 2H), 7.81 (d, J = 8.0 Hz, 1H), 7.63 (d, J = 8.0 Hz, 2H), 7.20 (d, J = 8.0 Hz, 1H), 7.14 (s, 1H), 3.97 (s, 3H), 3.91 (s, 3H), 2.62 (s, 3H); ^{13}C NMR (125 MHz, CDCl_3) δ 199.3, 166.9, 159.5, 145.6, 144.7, 131.3, 130.3, 129.9, 127.5, 127.4, 119.8, 110.7, 55.8, 52.4, 32.1; IR (neat cm^{-1}) 2997, 2955, 2929, 2845, 2162, 1714, 1657, 1604, 1554, 1280, 1247, 831, 768. HRMS (DART, $\text{M}^+ + \text{H}$) m/z 285.1111 (calculated for $\text{C}_{17}\text{H}_{17}\text{O}_4$, 285.1127).

1-(4'-Dimethylamino-3-methoxy-biphenyl-4-yl)-ethanone (15). According to the general Suzuki coupling procedure, ketone **7** (0.50 g, 2.18 mmol), *N,N*-dimethylamine phenylboronic acid (0.43 g, 2.62 mmol), Cs_2CO_3 (2.13 g, 6.54 mmol), $\text{Pd}(\text{PPh}_3)_2\text{Cl}_2$ (0.15 g, 0.22 mmol, 10% Pd), and anhydrous dioxane (8 mL) were added to a 50 mL screw-cap pressure vessel. The mixture was stirred, degassed by purging with argon for 15 min, and placed in an 80 °C oil bath for 12 h. Following the general workup and flash chromatography (SiO_2 , 20 g, 50% EtOAc/hexanes), ketone **15** was obtained as a yellow solid (0.42 g, 72%); TLC R_f = 0.41 (20% EtOAc/hexanes); mp 107.7–108.0 °C; ^1H NMR (500 MHz, chloroform-*d*) δ 7.80 (d, J = 8.1 Hz, 1H), 7.52 (d, J = 8.7 Hz, 2H), 7.17 (dd, J = 8.1, 1.4 Hz, 1H), 7.10 (s, 1H), 6.78 (d, J = 8.8 Hz, 2H), 3.96 (s, 3H), 3.00 (s, 6H), 2.62 (s, 3H); ^{13}C NMR (125 MHz, CDCl_3) δ 199.2, 159.8, 150.8, 147.2, 131.3, 128.1, 125.6, 118.6, 112.7, 109.3, 55.7, 40.6, 32.1; IR (neat cm^{-1}) 2894, 2816, 1657, 1588, 1564, 807; HRMS (DART, $\text{M}^+ + \text{H}$) m/z 270.1488 (calculated for $\text{C}_{17}\text{H}_{20}\text{NO}_2$, 270.1494).

1-(4'-Fluoro-3-methoxy-biphenyl-4-yl)-ethanone (16). According to the general Suzuki coupling procedure, ketone **7** (0.50 g, 2.18 mmol), 4-fluorophenylboronic acid (0.37 g, 2.62 mmol), Cs_2CO_3

(2.13 g, 6.54 mmol), $\text{Pd}(\text{PPh}_3)_2\text{Cl}_2$ (0.15 g, 0.22 mmol, 10% Pd), and anhydrous dioxane (8 mL) were added to a 50 mL screw-cap pressure vessel. The mixture was stirred, degassed by purging with argon for 15 min, sealed, and placed in an 80 °C oil bath for 12 h. Following the general workup and flash chromatography (SiO_2 , 20 g, 50% EtOAc/hexanes), ketone **16** was obtained as a white solid (0.49 g, 92%); TLC R_f = 0.52 (15% EtOAc/hexanes); mp 89.5–90.0 °C; ^1H NMR (500 MHz, chloroform-*d*) δ 7.83 (d, J = 8.0 Hz, 1H), 7.59–7.56 (m, 2H), 7.17–7.11 (m, 4H), 3.99 (s, 3H), 2.65 (s, 3H); ^{13}C NMR (125 MHz, CDCl_3) δ 199.2, 163.0 (d, J = 246.2 Hz, 1C), 159.6, 145.9, 136.4, 131.3, 129.0 (d, J = 7.5 Hz, 2C), 126.9, 119.4, 116.1 (d, J = 21.2 Hz, 2C), 110.4, 55.7, 32.1; IR (neat cm^{-1}) 3064, 3009, 1666, 1604, 1558, 841; HRMS (DART, $\text{M}^+ + \text{H}$) m/z 245.1002 (calculated for $\text{C}_{15}\text{H}_{14}\text{FO}_2$, 245.0978).

1-Biphenyl-4-yl-ethanone (17). According to the general Suzuki coupling procedure, 4'-bromoacetophenone **8** (0.600 g, 3.02 mmol), phenylboronic acid (0.736 g, 6.04 mmol), Cs_2CO_3 (2.95 g, 9.06 mmol), $\text{Pd}(\text{PPh}_3)_2\text{Cl}_2$ (0.211 g, 0.30 mmol, 10% Pd), and anhydrous dioxane (6 mL) were heated at 80 °C for 5 h. Following the general workup and flash chromatography (SiO_2 , 20 g, 5% EtOAc/hexanes), biaryl ketone **17** was obtained as a white solid (0.415 g, 70%); TLC R_f = 0.6 (25% EtOAc/hexanes); mp 118–120 °C; ^1H NMR (500 MHz, CDCl_3) δ 8.01 (d, J = 7.5 Hz, 2H), 7.67 (d, J = 7.5 Hz, 2H), 7.61 (d, J = 7.6 Hz, 2H), 7.46 (dd, J = 7.3 Hz, 7.3 Hz, 1H), 7.46 (dd, J = 7.3 Hz, 7.3 Hz, 1H), 7.40–7.37 (m, 1H), 2.62 (s, 3H); ^{13}C NMR (125 MHz, CDCl_3) δ 197.8, 145.8, 139.9, 136.0, 129.1, 129.1, 128.4, 127.4, 127.3, 26.8; IR (neat cm^{-1}) 3072, 2996, 2916, 2047, 1676, 1599, 1402, 958, 763; HRMS (DART, $\text{M}^+ + \text{H}$) m/z 197.0984 (calculated for $\text{C}_{14}\text{H}_{13}\text{O}$, 197.0966).

General Procedure for the Suzuki Coupling of Pyridine Compounds. **1-(6-Phenyl-pyridin-3-yl)-ethanone (40).** 5-Acetyl-2-bromopyridine **38** (0.656 g, 3.28 mmol), phenylboronic acid (0.800 g, 6.56 mmol), Na_2CO_3 (0.243 g, 2.29 mmol), $\text{Pd}(\text{PPh}_3)_2\text{Cl}_2$ (0.115 g, 0.16 mmol, 5% Pd), acetonitrile (26 mL), and H_2O (26 mL) were added to a 50 mL screw-cap pressure vessel. The mixture was stirred, degassed by purging with argon for 15 min, sealed, and placed in an 80 °C oil bath for 14 h (overnight). The dark colored mixture was cooled and extracted with ether. The organic layer was filtered through a pad of Celite, rinsed with ether, washed with brine, dried over MgSO_4 , and filtered. The filtrate was concentrated, and the residue purified by flash column chromatography (SiO_2 , 20 g, 5% EtOAc/hexanes) to afford the coupled ketone **40** as a white solid (0.33g, 52%); TLC R_f = 0.4 (25% EtOAc/hexanes); mp 124.9–126.2 °C; ^1H NMR (500 MHz, CDCl_3) δ 9.22 (d, J = 2.0 Hz, 1H), 8.28 (dd, J = 8.3, 2.2 Hz, 1H), 8.10–7.99 (m, 2H), 7.83 (d, J = 8.3 Hz, 1H), 7.55–7.40 (m, 3H), 2.65 (s, 3H); ^{13}C NMR (125 MHz, CDCl_3) δ 196.6, 161.1, 150.2, 138.2, 136.7, 130.9, 130.4, 129.2, 127.6, 120.4, 26.9; IR (neat cm^{-1}) 3062, 2999, 2960, 2322, 1673, 1557, 1382, 1016, 736; HRMS (DART, $\text{M}^+ + \text{H}$) m/z 198.0906 (calculated for $\text{C}_{13}\text{H}_{13}\text{NO}$, 198.0919).

1-(6-p-Tolyl-pyridin-3-yl)-ethanone (41). According to the general Suzuki coupling of pyridine compounds 5-acetyl-2-bromopyridine **38** (0.394 g, 1.97 mmol), 4-tolylboronic acid (0.535 g, 3.94 mmol), Na_2CO_3 (0.146 g, 1.38 mmol), $\text{Pd}(\text{PPh}_3)_2\text{Cl}_2$ (0.042 g, 0.06 mmol, 3% Pd), acetonitrile (7.8 mL), and water (7.8 mL) were heated at 80 °C for 14 h (overnight). Following the general workup and flash chromatography (SiO_2 , 20 g, 5% EtOAc/hexanes), coupled ketone was obtained as a white solid **41** (0.381 g, 92%); TLC R_f = 0.4 (25% EtOAc/hexanes); mp 106–107.5 °C; ^1H NMR (500 MHz, CDCl_3) δ 9.19 (d, J = 2.2 Hz, 1H), 8.24 (dd, J = 8.3, 2.3 Hz, 1H), 7.95 (d, J = 8.2 Hz, 2H), 7.79 (d, J = 8.4 Hz, 1H), 7.29 (d, J = 8.4 Hz, 2H), 2.63 (s, 3H), 2.40 (s, 3H); ^{13}C NMR (125 MHz, CDCl_3) δ 196.6, 161.0, 150.2, 140.5, 136.4, 135.5, 130.5, 129.8, 127.4, 26.8, 21.5; IR (neat cm^{-1}) 3024, 2911, 2853, 2042, 1671, 1589, 1555, 1371, 1279, 1141, 819, 762; HRMS (DART, $\text{M}^+ + \text{H}$) m/z 212.1093 (calculated for $\text{C}_{14}\text{H}_{14}\text{NO}$, 212.1075).

General Procedure for the Suzuki Coupling of Pyrimidine Compounds. **1-(2-Phenyl-pyrimidin-5-yl)-ethanone (42).** Ketone **39** (0.72 g, 4.6 mmol), phenylboronic acid (0.841 g, 6.9 mmol), $\text{Pd}(\text{OAc})_2$ (0.041 g, 0.184 mmol, 4% Pd), PPh_3 (0.241 g, 0.92 mmol), sat. Na_2CO_3 (23 mL), and anhydrous dioxane (30 mL) were added to

a 100 mL screw-cap pressure vessel. The mixture was stirred, degassed by purging with argon for 15 min, sealed, and placed in a 110 °C oil bath for 14 h. The dark colored mixture was cooled and extracted with ether. The organic layer was filtered through a pad of Celite, rinsed with ether, washed with brine, dried over MgSO_4 , and filtered. The filtrate was concentrated and the residue purified by flash column chromatography (SiO_2 , 20 g, 5% EtOAc/hexanes) to afford the coupled ketone **42** as a white solid (0.66 g, 74%): TLC R_f = 0.4 (25% EtOAc/hexanes); mp 154–156 °C; ^1H NMR (500 MHz, CDCl_3) δ 9.23 (s, 2H), 8.49 (dd, J = 8.1, 1.6 Hz, 2H), 7.72–7.36 (m, 3H), 2.61 (s, 3H); ^{13}C NMR (125 MHz, CDCl_3) δ 195.2, 167.2, 157.5, 136.7, 132.1, 130.0, 128.9, 127.4, 26.8; IR (neat cm^{-1}) 3077, 3036, 2049, 1681, 1537, 1429, 1376, 1271, 954, 744, 688; HRMS (DART, M^+ + H) m/z 199.0868 (calculated for $\text{C}_{12}\text{H}_{11}\text{N}_2\text{O}$, 199.0871).

General Procedure for Wittig Homologation/Enol Ether Hydrolysis/Ohira–Bestmann Homologation. *3-Methoxy-4-(1-methyl-prop-2-ynyl)-biphenyl (18).* A 50 mL round bottomed flask with a stir bar was flame-dried under argon and allowed to cool to room temperature. Methoxymethyl triphenylphosphonium chloride (1.23 g 3.6 mmol) was added to the flask, followed by dry THF (9.7 mL) and cooled to 0 °C. To the cold suspension was added NaO^tBu (0.434 g, 4.5 mmol) in one portion and stirred for 0.5 h at 0 °C. Ketone **9** (0.409 g, 1.8 mmol) in THF (3 mL) was added dropwise to the red-orange suspension and allowed to stir for 20 min. The reaction was followed by TLC and quenched with water and diluted with ether. The organic phase was separated and the aqueous phase extracted with ether. The combined extracts were washed with brine, dried over MgSO_4 , and filtered. The filtrate was concentrated and passed through a column of silica gel to afford a mixture of enol ethers (0.409 g) that were immediately hydrolyzed in the subsequent step.

To a solution of 0.409 g (1.6 mmol) of enol ether in THF/ H_2O (9:1, 6 mL), which was degassed by purging with argon, $\text{Hg}(\text{OAc})_2$ (1.54 g, 4.8 mmol) was added. The reaction mixture was stirred for 2 h under argon at RT and then 5 mL of saturated solution of KI was added, stirred for 15 min. The reaction mixture was then extracted with ether, and the combined extracts were washed with a saturated solution of NaHCO_3 , sat. $\text{Na}_2\text{S}_2\text{O}_3$, and brine, dried over MgSO_4 , and filtered. The filtrate was concentrated to afford the aldehyde (0.107 g) as a colorless oil, which was taken to the next step without further purification.

Aldehyde (0.1 g 0.41 mmol) in MeOH (3 mL) under argon was cooled to 0 °C, and the Ohira–Bestmann reagent (0.120 g, 0.62 mmol) dissolved in MeOH (1 mL) was added. Powdered K_2CO_3 (0.12 g, 0.87 mmol) was added to the homogeneous pale greenish solution and stirred for 2 h. The reaction was followed by TLC and diluted with water, and the aqueous phase was extracted with ether. The combined organic extracts were washed with brine, dried over MgSO_4 , and filtered. The filtrate was concentrated and purified by flash column chromatography (SiO_2 , 10 g, 2% EtOAc/hexanes) to afford acetylene **18** as a colorless oil (0.034g, 10% yield over 3 steps): TLC R_f = 0.3 (2% EtOAc/hexanes); ^1H NMR (500 MHz, CDCl_3) δ 7.64 (d, J = 7.8 Hz, 1H), 7.59 (d, J = 7.2 Hz, 2H), 7.44 (dd, J = 7.6 Hz, 7.6 Hz, 1H), 7.44 (dd, J = 7.6 Hz, 7.6 Hz, 1H), 7.35 (m, 1H), 7.20 (dd, J = 7.8, 1.4 Hz, 1H), 7.06 (s, 1H), 4.23 (qd, J = 7.0, 2.4 Hz, 1H), 3.91 (s, 3H), 2.24 (d, J = 2.5 Hz, 1H), 1.49 (d, J = 7.1 Hz, 3H); ^{13}C NMR (125 MHz, CDCl_3) δ 156.5, 141.5, 141.5, 130.3, 128.9, 128.2, 127.5, 127.4, 119.8, 109.7, 87.8, 69.6, 55.7, 25.4, 22.9; IR (neat cm^{-1}) 3290, 3029, 2972, 2931, 2107, 1608, 1566, 1484, 1402, 1220, 1036, 761, 698, 642; HRMS (DART, M^+ + H) m/z 237.1264 (calculated for $\text{C}_{17}\text{H}_{17}\text{O}$, 237.1279).

4-[3-Methoxy-4-(1-methyl-prop-2-ynyl)-phenyl]-pyridine (19). According to the general procedure for homologation, methoxymethyl triphenylphosphonium chloride (1.208 g, 3.52 mmol) in dry THF (4 mL), NaO^tBu (0.432 g, 4.4 mmol), and ketone **10** (0.400 g, 1.76 mmol) in THF (3 mL) were stirred at 0 °C. Following the general workup, the mixture of enol ethers 0.350 g (1.37 mmol) in THF/ H_2O (9:1, 6 mL) was hydrolyzed using $\text{Hg}(\text{OAc})_2$ (1.30 g, 4.1 mmol) at room temperature. After the general extraction procedure, aldehyde (0.330 g, 1.36 mmol) in MeOH (3 mL), the Ohira–Bestmann reagent (0.422 g, 2.0 mmol) dissolved in MeOH (1 mL), and powdered

K_2CO_3 (0.337 g, 2.70 mmol) were stirred at 0 °C. Following the general workup and flash chromatography (SiO_2 , 15g, 25% EtOAc/hexanes), alkyne **19** was obtained as a pale yellow solid (0.100 g, 23% yield over 3 steps). TLC R_f = 0.1 (25% EtOAc/hexanes); mp 111.6–113.6 °C; ^1H NMR (500 MHz, CDCl_3) δ 8.64 (d, J = 7.6 Hz, 2H), 7.67 (d, J = 7.9 Hz, 1H), 7.49 (d, J = 6.0 Hz, 2H), 7.07 (d, J = 1.3 Hz, 1H), 4.21 (qd, J = 7.0, 2.5 Hz, 1H), 3.91 (s, 3H), 2.27–2.21 (m, 1H), 1.47 (d, J = 7.1 Hz, 3H); ^{13}C NMR (125 MHz, CDCl_3) δ 156.5, 150.1, 148.5, 138.0, 132.2, 128.4, 121.7, 119.5, 109.0, 87.1, 70.0, 55.6, 25.3, 22.6; IR (neat cm^{-1}) 3156, 3042, 2930, 2099, 1596, 1454, 1227, 1032, 810; HRMS (DART, M^+ + H) m/z 238.1259 (calculated for $\text{C}_{16}\text{H}_{16}\text{NO}$, 238.1232).

3'-Methoxy-4'-(1-methyl-prop-2-ynyl)-biphenyl-4-ol (20). According to the general procedure for homologation, methoxymethyl triphenylphosphonium chloride (4.71 g, 13.73 mmol) in dry THF (37 mL), NaO^tBu (1.58 g, 16.5 mmol), and ketone **11** (1.79 g, 5.49 mmol) in THF (7 mL) were stirred at 0 °C. Following the general workup, the mixture of enol ethers (1.77 g, 5.00 mmol) in THF/ H_2O (9:1, 17 mL) was hydrolyzed using $\text{Hg}(\text{OAc})_2$ (4.8 g, 14.97 mmol) at room temperature. After the general extraction procedure, aldehyde (1.564 g, 4.65 mmol) in MeOH (20 mL), the Ohira–Bestmann reagent (1.60 g, 8.4 mmol) dissolved (11 mL) in MeOH, and powdered K_2CO_3 (1.337 g, 9.7 mmol) were stirred at 0 °C. Following the general workup and flash chromatography (SiO_2 , 30 g, 15% EtOAc/hexanes), O-THP alkyne was obtained as a pale white solid (0.84 g). Deprotection of O-THP alkyne was carried out by dissolving the protected alkyne (0.84 g, 2.5 mmol) in MeOH (150 mL) and cooled to 0 °C. *p*-Toluenesulfonic acid (0.951 g, 2.5 mmol) was added and the reaction allowed to warm to room temperature. The reaction was followed by TLC, diluted with water, neutralized with sat NaHCO_3 , and extracted with ether. The organic extracts were washed with brine, dried over MgSO_4 , and filtered. The filtrate was concentrated and purified by flash column chromatography (SiO_2 , 30g, 15% EtOAc/hexanes) to give the terminal acetylene **20** as a white solid (0.61 g, 43% yield over 4 steps); TLC R_f = 0.3 (25% EtOAc/hexanes); mp 90.2–91 °C; ^1H NMR (500 MHz, CDCl_3) δ 7.57 (d, J = 7.9 Hz, 1H), 7.45 (d, J = 8.6 Hz, 2H), 7.11 (dd, J = 7.9, 1.7 Hz, 1H), 6.98 (d, J = 1.6 Hz, 1H), 6.88 (d, J = 8.6 Hz, 2H), 4.18 (qd, J = 7.0, 2.4 Hz, 1H), 3.88 (s, 3H), 2.20 (d, J = 2.5 Hz, 1H), 1.45 (d, J = 7.0 Hz, 3H); ^{13}C NMR (125 MHz, CDCl_3) δ 156.5, 155.3, 141.0, 134.3, 129.7, 128.6, 128.2, 119.4, 115.8, 109.3, 87.8, 69.5, 55.7, 25.3, 22.9; IR (neat cm^{-1}) 3334, 3300, 2938, 1606, 1494, 1218, 807, 633; HRMS (DART, M^+ + H) m/z 253.1224 (calculated for $\text{C}_{17}\text{H}_{17}\text{O}_2$, 253.1229).

3-Methoxy-4'-methyl-4-(1-methyl-prop-2-ynyl)-biphenyl (21). According to the general procedure for homologation, methoxymethyl triphenylphosphonium chloride (1.07 g, 3.12 mmol) in dry THF (9 mL), NaO^tBu (0.37g, 3.9 mmol), and ketone **12** (0.376 g, 1.56 mmol) in THF (3 mL) were stirred at 0 °C. Following the general workup, the mixture of enol ethers (0.375 g, 1.39 mmol) in THF/ H_2O (9:1, 5 mL) was hydrolyzed using $\text{Hg}(\text{OAc})_2$ (1.30g, 4.1 mmol) at room temperature. After the general extraction procedure, aldehyde (0.141 g 0.60 mmol) in MeOH (3 mL), the Ohira–Bestmann reagent (0.160 g, 0.83 mmol) dissolved in MeOH (1 mL), and powdered K_2CO_3 (0.161 g, 1.16 mmol) were stirred at 0 °C. Following the general workup and flash chromatography (SiO_2 , 6 g, 2% EtOAc/hexanes), alkyne **21** was obtained as a colorless oil (0.017 g, 5% yield over 3 steps); TLC R_f = 0.2 (2% EtOAc/hexanes); ^1H NMR (500 MHz, CDCl_3) δ 7.60 (d, J = 7.8 Hz, 1H), 7.47 (d, J = 8.1 Hz, 2H), 7.24 (d, J = 7.8 Hz, 2H), 7.17 (dd, J = 7.8, 1.6 Hz, 1H), 7.03 (d, J = 1.5 Hz, 1H), 4.20 (qd, J = 7.0, 2.4 Hz, 1H), 3.89 (s, 3H), 2.39 (s, 3H), 2.21 (d, J = 2.5 Hz, 1H), 1.47 (d, J = 7.1 Hz, 3H); ^{13}C NMR (125 MHz, CDCl_3) δ 156.5, 141.4, 138.6, 137.3, 129.9, 129.7, 128.1, 127.2, 119.6, 109.5, 87.8, 69.5, 55.7, 25.3, 22.9, 21.3; IR (neat cm^{-1}) 3305, 3028, 2970, 2932, 2357, 1607, 1582, 1225, 1031, 804; HRMS (DART, M^+ + H) m/z 251.1422 (calculated for $\text{C}_{18}\text{H}_{19}\text{O}$, 251.1436).

3'-Methoxy-4'-(1-methyl-prop-2-ynyl)-biphenyl-4-carbonitrile (22). According to general procedure for homologation, methoxymethyl triphenylphosphonium chloride (1.09 g, 3.18 mmol) in dry THF (4 mL), NaO^tBu (0.382 g, 3.9 mmol), and ketone **13** (0.400 g, 1.59 mmol) in THF (3 mL) were stirred at 0 °C. Following the

general workup, the mixture of enol ethers (0.330 g, 1.18 mmol) in THF/H₂O (9:1, 5 mL) was hydrolyzed using Hg(OAc)₂ (1.13g, 3.5 mmol) at room temperature. After the general extraction procedure, aldehyde (0.285 g, 1.1 mmol) in MeOH (3 mL), the Ohira–Bestmann reagent (0.442 g, 2.15 mmol) dissolved in MeOH (1 mL), and powdered K₂CO₃ (0.370 g, 2.68 mmol) were stirred at 0 °C. Following the general workup and flash chromatography (SiO₂, 10 g, 5% EtOAc/hexanes), alkyne **22** was obtained as a white solid (0.200 g, 47% yield over 3 steps); TLC R_f = 0.2 (5% EtOAc/hexanes); mp 103.7–104 °C; ¹H NMR (500 MHz, CDCl₃) δ 7.72 (m, 2H), 7.67 (m, 3H), 7.19 (d, J = 7.9 Hz, 1H), 7.03 (s, 1H), 4.23 (q, J = 7.0, 1H), 3.92 (s, 3H), 2.25 (d, J = 2.4 Hz, 1H), 1.48 (d, J = 7.0 Hz, 3H); ¹³C NMR (125 MHz, CDCl₃) δ 156.7, 145.8, 139.3, 132.7, 131.9, 128.6, 127.9, 119.9, 119.9, 119.1, 111.1, 109.5, 87.3, 69.9, 55.8, 25.4, 22.8; IR (neat cm⁻¹) 3285, 3069, 2935, 2221, 1604, 1488, 1393, 1225, 1024, 807, 657; HRMS (DART, M⁺ + H) m/z 262.1253 (calculated for C₁₈H₁₆NO, 262.1232).

Carbamic acid 3'-methoxy-4'-(1-methyl-prop-2-ynyl)-biphenyl-4-yl ester (23). To a 25 mL flame-dried flask with a stir bar cooled to room temperature was added alkyne **20** (0.115 g, 0.46 mmol) dissolved in anhydrous CH₂Cl₂. The reactant was cooled to 0 °C, and chlorosulfonyl isocyanate (0.08 mL, 0.92 mmol) was added dropwise. After 15 min, the reaction mixture was brought to room temperature and followed by TLC. The reaction was quenched with water and extracted with ether. The organic extracts were washed with brine, dried over MgSO₄, and filtered. The filtrate was concentrated and purified by flash column chromatography (SiO₂, 7 g, 25% EtOAc/hexanes) to give the terminal acetylene **23** as a white solid (0.092 g, 68% yield); TLC R_f = 0.1 (25% EtOAc/hexanes); mp 113.6–115.3 °C; ¹H NMR (500 MHz, CDCl₃) δ 7.61 (d, J = 7.8 Hz, 1H), 7.56 (d, J = 8.5 Hz, 2H), 7.19 (d, J = 8.5 Hz, 2H), 7.15 (dd, J = 7.8, 1.4 Hz, 1H), 7.01 (d, J = 1.7 Hz, 1H), 4.21 (qd, J = 7.0, 2.3 Hz, 1H), 3.88 (s, 3H), 2.23 (d, J = 2.4 Hz, 1H), 1.47 (d, J = 7.0 Hz, 3H); ¹³C NMR (125 MHz, CDCl₃) δ 189.2, 156.4, 155.6, 150.3, 140.6, 138.9, 133.1, 130.3, 128.3, 128.2, 122.1, 119.7, 109.6, 87.7, 69.6, 60.6, 55.7, 25.3, 22.8, 21.2, 14.4; IR (neat cm⁻¹) 3423, 3308, 3268, 3199, 2969, 2341, 2105, 1698, 1606, 1494, 1378, 1213, 586; HRMS (DART, M⁺ + H) m/z 296.1300 (calculated for C₁₈H₁₈NO₃, 296.1287).

3'-Methoxy-4'-(1-methyl-prop-2-ynyl)-biphenyl-4-carboxylic Acid Methyl Ester (24). According to the general procedure for homologation, methoxymethyl triphenylphosphonium chloride (1.05 g, 3.06 mmol) in dry THF (9 mL), NaO^tBu (0.367 g, 3.9 mmol), and ketone **14** (0.434 g, 1.59 mmol) in THF (3 mL) were stirred at 0 °C. Following the general workup, the mixture of enol ethers (0.214 g, 0.69 mmol) in THF/H₂O (9:1, 5 mL) was hydrolyzed using Hg(OAc)₂ (0.656 g, 2.1 mmol) at room temperature. After the general extraction procedure, aldehyde (0.194 g, 0.65 mmol) in MeOH (3 mL), the Ohira–Bestmann reagent (0.224 g, 1.17 mmol) dissolved in MeOH (2 mL), and powdered K₂CO₃ (0.188 g, 1.36 mmol) were stirred at 0 °C. Following the general workup and flash chromatography (SiO₂, 7 g, 2% EtOAc/hexanes), alkyne **24** was obtained as a white solid (0.111 g, 25% yield over 3 steps); TLC R_f = 0.3 (5% EtOAc/hexanes); mp 106–108.5 °C; ¹H NMR (500 MHz, CDCl₃) δ 8.09 (d, J = 8.1 Hz, 2H), 7.72–7.57 (m, 3H), 7.20 (d, J = 7.7 Hz, 1H), 7.06 (s, 1H), 4.21 (q, J = 5.0 Hz, 1H), 3.92 (s, 3H), 3.90 (s, 3H), 2.23 (d, J = 2.0 Hz, 1H), 1.47 (d, J = 7.0 Hz, 3H); ¹³C NMR (125 MHz, CDCl₃) δ 167.1, 156.5, 145.8, 140.1, 131.3, 130.2, 129.1, 128.4, 127.2, 119.9, 109.5, 87.5, 69.7, 55.7, 52.3, 25.4, 22.8; IR (neat cm⁻¹) 3255, 2970, 2950, 2929, 2108, 1698, 1605, 1430, 1393, 1104, 1281, 769, 676; HRMS (DART, M⁺ + H) m/z 295.1329 (calculated for C₁₉H₁₉O₃, 295.1334).

3'-Methoxy-4'-(1-methyl-prop-2-ynyl)-biphenyl-4-yl)-dimethylamine (25). According to the general procedure for homologation, methoxymethyl triphenylphosphonium chloride (0.67 g, 1.95 mmol) in dry THF (10 mL), NaO^tBu (0.22 g, 2.34 mmol), and ketone (0.21 g, 0.78 mmol) in THF (3 mL) were stirred at 0 °C. Following the general workup, the mixture of enol ethers (0.18 g, 0.62 mmol) in THF/H₂O (9:1, 10 mL) was hydrolyzed using Hg(OAc)₂ (0.30 g, 0.93 mmol) at room temperature. After the general extraction procedure, aldehyde (0.17 g, 0.62 mmol) in dry MeOH (6 mL), the

Ohira–Bestmann reagent (0.36 g, 1.86 mmol) dissolved in MeOH (2 mL), and powdered K₂CO₃ (0.26 g, 1.86 mmol) were stirred at 0 °C. Following the general workup and flash chromatography (SiO₂, 10g, 15% EtOAc/hexanes), alkyne **25** was obtained as a white solid (0.015 g, 6% yield over 3 steps); TLC R_f = 0.52 (10% EtOAc/hexanes); mp 60.8–61.1 °C; ¹H NMR (500 MHz, chloroform-d) δ 7.56 (d, J = 7.9 Hz, 1H), 7.48 (d, J = 8.9 Hz, 2H), 7.14 (dd, J = 7.9, 1.7 Hz, 1H), 7.01 (d, J = 1.6 Hz, 1H), 6.79 (d, J = 8.7 Hz, 2H), 4.18 (qd, J = 7.1, 2.6 Hz, 2H), 3.88 (s, 3H), 2.98 (s, 6H), 2.20 (d, J = 2.5 Hz, 1H), 1.46 (d, J = 7.1 Hz, 3H); ¹³C NMR (125 MHz, CDCl₃) δ 156.4, 150.2, 141.5, 129.5, 128.9, 128.0, 127.9, 118.9, 112.9, 108.9, 88.0, 69.4, 55.6, 40.8, 25.3, 22.9; IR (neat cm⁻¹) 3292, 2972, 2932, 1605, 1574, 1397, 804; HRMS (DART, M⁺ + H) m/z 280.1703 (calculated for C₁₉H₂₂NO, 280.1701).

4-Fluoro-3-methoxy-4-(1-methyl-prop-2-ynyl)-biphenyl (26). According to the general procedure for homologation, methoxymethyl triphenylphosphonium chloride (1.70 g, 4.97 mmol) in dry THF (10 mL), NaO^tBu (0.57 g, 5.97 mmol), and ketone (0.49 g, 1.99 mmol) in THF (3 mL) were stirred at 0 °C. Following the general workup, the mixture of enol ethers (0.51 g, 1.87 mmol) in THF/H₂O (9:1, 10 mL) was hydrolyzed using Hg(OAc)₂ (1.78 g, 5.61 mmol) at room temperature. After the general extraction procedure, aldehyde (0.48 g, 1.87 mmol) in dry MeOH (6 mL), the Ohira–Bestmann reagent (0.72 g, 3.74 mmol) dissolved in MeOH (2 mL), and powdered K₂CO₃ (0.78 g, 5.61 mmol) were stirred at 0 °C. Following the general workup and flash chromatography (SiO₂, 30g, 15% EtOAc/hexanes), alkyne **26** was obtained as a white solid (0.23 g, 45% yield over 3 steps); TLC R_f = 0.41 (10% EtOAc/hexane); mp 57.8–58.0 °C; ¹H NMR (500 MHz, chloroform-d) δ 7.62 (d, J = 7.8 Hz, 1H), 7.56–7.49 (m, 2H), 7.15–7.08 (m, 3H), 6.99 (d, J = 1.7 Hz, 1H), 4.21 (qd, J = 7.0, 2.4 Hz, 1H), 3.90 (s, 3H), 2.23 (d, J = 2.5 Hz, 1H), 1.48 (d, J = 7.1 Hz, 3H); ¹³C NMR (125 MHz, CDCl₃) δ 162.6 (d, J = 245.0 Hz, 1C); 156.5, 140.5, 137.5, 130.3, 128.8 (d, J = 7.5 Hz, 2C), 128.3, 119.7, 115.7 (d, J = 21.2 Hz, 2C), 109.5, 87.7, 69.6, 55.7, 25.3, 22.8; IR (neat cm⁻¹) 3306, 3297, 2975, 2957, 2931, 1607, 1492; HRMS (DART, M⁺ + H) m/z 255.1199 (calculated for C₁₇H₁₆FO, 255.1185).

4-(1-Methyl-prop-2-ynyl)-biphenyl (27). According to the general procedure for homologation, methoxymethyl triphenylphosphonium chloride (1.16g, 3.4 mmol) in dry THF (10 mL), NaO^tBu (0.409 g, 4.2 mmol), and ketone **17** (0.330 g, 1.70 mmol) in THF (3 mL) were stirred at 0 °C. Following the general workup, the mixture of enol ethers (0.388 g, 1.73 mmol) in THF/H₂O (9:1, 6 mL) was hydrolyzed using Hg(OAc)₂ (1.650 g, 5.2 mmol) at room temperature. After the general extraction procedure, aldehyde (0.150 g, 0.71 mmol) in MeOH (3 mL), the Ohira–Bestmann reagent (0.205 g, 1.07 mmol) dissolved in MeOH (2 mL), and powdered K₂CO₃ (0.207 g, 1.49 mmol) were stirred at 0 °C. Following the general workup and flash chromatography (SiO₂, 5 g, 2% EtOAc/hexanes), alkyne **27** was obtained as a colorless oil (0.034 g, 24% yield over 3 steps); TLC R_f = 0.3 (2% EtOAc/hexanes); ¹H NMR (500 MHz, CDCl₃) δ 7.70–7.53 (m, 4H), 7.52–7.41 (m, 4H), 7.36–7.33 (m, 1H), 3.83 (qd, J = 7.2, 2.4 Hz, 1H), 2.30 (d, J = 2.5 Hz, 1H), 1.57 (d, J = 7.2 Hz, 3H); ¹³C NMR (125 MHz, CDCl₃) δ 141.9, 141.1, 140.0, 128.9, 127.6, 127.4, 127.3, 87.3, 70.5, 31.5, 24.4; IR (neat cm⁻¹) 3288, 3032, 2974, 2869, 2111, 1595, 1293, 835, 762, 627, 531; HRMS (DART, M⁺ + H) m/z 207.1161 (calculated for C₁₆H₁₅, 207.1174).

5-(1-Methyl-prop-2-ynyl)-2-phenyl-pyridine (43). According to general procedure for homologation, methoxymethyl triphenylphosphonium chloride (1.01 g, 2.94 mmol) in dry THF (9 mL), NaO^tBu (0.353 g, 3.7 mmol), and ketone **40** (0.290 g, 1.47 mmol) in THF (3 mL) were stirred at 0 °C. Following the general workup, the mixture of enol ethers (0.298 g, 1.33 mmol) in THF/H₂O (9:1, 5 mL) was hydrolyzed using Hg(OAc)₂ (1.272 g, 3.9 mmol) at room temperature. After the general extraction procedure, aldehyde (0.175 g, 0.83 mmol) in MeOH (4 mL), the Ohira–Bestmann reagent (0.238 g, 1.24 mmol) dissolved in MeOH (2 mL), and powdered K₂CO₃ (0.240 g, 1.74 mmol) were stirred at 0 °C. Following the general workup and flash chromatography (SiO₂, 5g, 2% EtOAc/hexanes), alkyne **43** was obtained as a white solid (0.102 g, 34% yield over 3 steps); TLC R_f = 0.3 (5% EtOAc/hexanes); mp 90.3–92 °C; ¹H NMR (500 MHz,

CDCl_3) δ 8.67 (d, J = 2.3 Hz, 1H), 7.97–7.95 (m, 2H), 7.79 (dd, J = 8.2, 2.3 Hz, 1H), 7.68 (d, J = 8.2 Hz, 1H), 7.49–7.42 (m, 2H), 7.42–7.36 (m, 1H), 3.83 (qd, J = 7.2, 2.5 Hz, 1H), 2.30 (d, J = 2.5 Hz, 1H), 1.55 (d, J = 7.2 Hz, 3H); ^{13}C NMR (125 MHz, CDCl_3) δ 156.3, 148.6, 139.3, 136.6, 135.3, 129.0, 128.9, 127.0, 120.5, 85.9, 71.1, 29.2, 24.2; IR (neat cm^{-1}) 3292, 2976, 2930, 2870, 2325, 2107, 1594, 1473, 1293, 1018, 841, 740, 693, 644; HRMS (DART, M^+ + H) m/z 208.1144 (calculated for $\text{C}_{15}\text{H}_{14}\text{N}$, 208.1126).

5-(1-Methyl-prop-2-ynyl)-2-p-tolyl-pyridine (44). According to the general procedure for homologation, methoxymethyl triphenylphosphonium chloride (4.47 g, 3.61 mmol) in dry THF (10 mL), NaO^tBu (0.434 g, 4.5 mmol), and ketone **41** (0.381 g, 1.81 mmol) in THF (5 mL) were stirred at 0 °C. Following the general workup, the mixture of enol ethers (0.418 g, 1.75 mmol) in THF/ H_2O (9:1, 6 mL) was hydrolyzed using $\text{Hg}(\text{OAc})_2$ (1.670 g, 5.26 mmol) at room temperature. After the general extraction procedure, aldehyde (0.197 g, 0.87 mmol) in MeOH (4 mL), the Ohira–Bestmann reagent (0.252 g, 1.31 mmol) dissolved in MeOH (2 mL), and powdered K_2CO_3 (0.254 g, 1.84 mmol) were stirred at 0 °C. Following the general workup and flash chromatography (SiO_2 , 7 g, 2% EtOAc/hexanes), alkyne **44** was obtained as a pale yellow solid (0.140 g, 33% yield over 3 steps): TLC R_f = 0.3 (5% EtOAc/hexanes); mp 84.1–84.2 °C; ^1H NMR (500 MHz, CDCl_3) δ 8.65 (d, J = 2.3 Hz, 1H), 7.86 (d, J = 8.2 Hz, 2H), 7.77 (dd, J = 8.2, 2.3 Hz, 1H), 7.66 (d, J = 8.2 Hz, 1H), 7.26 (d, J = 7.9 Hz, 2H), 3.82 (qd, J = 7.1, 2.5 Hz, 1H), 2.39 (s, 3H), 2.29 (d, J = 2.5 Hz, 1H), 1.54 (d, J = 7.2 Hz, 3H); ^{13}C NMR (125 MHz, CDCl_3) δ 156.3, 148.6, 139.1, 136.6, 136.3, 135.3, 129.7, 126.9, 120.2, 86.1, 71.0, 29.3, 24.2, 21.5; IR (neat cm^{-1}) 3214, 2973, 2928, 2867, 2109, 1679, 1474, 1386, 1293, 1087, 1014, 818, 764, 697, 534; HRMS (DART, M^+ + H) m/z 222.1303 (calculated for $\text{C}_{16}\text{H}_{16}\text{N}$, 222.1283).

5-(1-Methyl-prop-2-ynyl)-2-phenyl-pyrimidine (45). According to the general procedure for homologation, methoxymethyl triphenylphosphonium chloride (2.3 g, 6.62 mmol) in dry THF (18 mL), NaO^tBu (0.797 g, 8.3 mmol), and ketone **42** (0.655 g, 3.31 mmol) in THF (6 mL) were stirred at 0 °C. Following the general workup, the mixture of enol ethers (0.398 g, 1.76 mmol) in THF/ H_2O (9:1, 6 mL) was hydrolyzed using $\text{Hg}(\text{OAc})_2$ (1.680 g, 5.28 mmol) at room temperature. After the general extraction procedure, aldehyde (0.300 g, 1.41 mmol) in MeOH (4 mL), the Ohira–Bestmann reagent (0.407 g, 2.12 mmol) dissolved in MeOH (2 mL), and powdered K_2CO_3 (0.410 g, 2.96 mmol) were stirred at 0 °C. Following the general workup and flash chromatography (SiO_2 , 5 g, 5% EtOAc/hexanes), alkyne **45** was obtained as a white solid (0.066 g, 10% yield over 3 steps): TLC R_f = 0.3 (5% EtOAc/hexanes); mp 75.4–76.7 °C; ^1H NMR (500 MHz, CDCl_3) δ 8.82 (s, 2H), 8.60–8.21 (m, 2H), 7.48–7.46 (m, 3H), 3.82 (qd, J = 7.1, 2.5 Hz, 1H), 2.34 (d, J = 2.5 Hz, 1H), 1.57 (d, J = 7.2 Hz, 3H); ^{13}C NMR (125 MHz, CDCl_3) δ 163.7, 156.1, 137.6, 133.3, 130.9, 128.8, 128.3, 84.6, 71.9, 27.4, 23.8; IR (neat cm^{-1}) 3205, 3059, 2978, 2934, 1584, 1547, 1425, 1296, 1175, 1094, 1069, 749, 692, 651; HRMS (DART, M^+ + H) m/z 209.1103 (calculated for $\text{C}_{14}\text{H}_{13}\text{N}_2$, 209.1079).

General Procedure for Sonogashira Coupling. **6-Ethyl-5-[3-(3-methoxy-biphenyl-4-yl)-but-1-ynyl]-pyrimidine-2,4-diamine (28).** To a 30 mL screw-cap vial was added ethyl-iodopyrimidine (0.347 g, 0.13 mmol), freshly purified CuI (0.005 g, 0.03 mmol), and $\text{Pd}(\text{PPh}_3)_2\text{Cl}_2$ (0.009 g, 0.01 mmol). Argon-purged anhydrous DMF (0.3 mL) was added followed by alkyne **18** (0.0342 g, 0.14 mmol). The reaction mixture was stirred under argon for 5 min followed by argon-purged anhydrous triethylamine. The reaction mixture was degassed once using the freeze/pump/thaw method. The vial was sealed under argon and heated at 60 °C for 14 h (overnight). At the end of the reaction, the dark reddish brown solution was concentrated and the product purified by flash column chromatography (SiO_2 , 10g, 2% MeOH/ CH_2Cl_2) to afford the coupled pyrimidine **28** as a pale yellow oil (0.035 g, 72% yield). The small amount of yellow oil was subjected to reverse phase chromatography (NH_2 capped SiO_2 , 2g, 100% CH_2Cl_2) to afford a colorless hygroscopic solid for biological evaluation. TLC R_f = 0.1 (5% MeOH/ CH_2Cl_2); ^1H NMR (500 MHz, CDCl_3) δ 7.59–7.56 (m, 3H), 7.42 (dd, J = 7.6, 7.6 Hz, 1H), 7.42 (dd, J = 7.6, 7.6 Hz, 1H), 7.37–7.30 (m, 1H), 7.18 (dd, J = 1.5, 7.8 Hz,

1H), 7.07 (s, 1H), 5.18 (s, 2H), 4.86 (s, 2H), 4.43 (q, J = 6.9 Hz, 1H), 3.92 (s, 3H), 2.70 (q, J = 7.6 Hz, 2H), 1.54 (d, J = 7.0 Hz, 3H), 1.24 (t, J = 7.6 Hz, 3H); ^{13}C NMR (125 MHz, CDCl_3) δ 173.5, 164.5, 160.8, 156.6, 141.5, 130.8, 128.9, 128.1, 127.6, 127.3, 119.8, 109.8, 102.3, 91.1, 74.6, 55.7, 29.9, 26.9, 23.1, 12.8; IR (neat cm^{-1}) 3459, 3372, 3304, 3160, 2970, 2930, 2870, 1967, 1547, 1435, 1219, 761, 696. HRMS (ESI, M^+ + H) m/z 373.2012 (calculated for $\text{C}_{23}\text{H}_{25}\text{N}_4\text{O}$, 373.2023). HPLC (a) t_R = 22.9 min, 99.3%; (b) t_R = 20.9 min, 98.9%.

6-Ethyl-5-[3-(2-methoxy-4-pyridin-4-yl-phenyl)-but-1-ynyl]-pyrimidine-2,4-diamine (29). According to the general Sonogashira coupling procedure, ethyl-iodopyrimidine (0.070 g, 0.26 mmol) CuI (0.0075 g, 0.039 mmol, 15 mol %), $\text{Pd}(\text{PPh}_3)_2\text{Cl}_2$ (0.019 g, 0.026 mmol, 10 mol %), and alkyne **19** (0.094 g, 0.40 mmol) were reacted in DMF/ Et_3N (1 mL each) at 70 °C for 12 h. After the mixture was cooled, the dark reddish brown solution was concentrated, and the product was purified by flash chromatography (SiO_2 , 10 g, 3% MeOH/ CH_2Cl_2) to afford coupled pyrimidine **29** as a pale white powder (0.085 g, 86%) followed by reverse phase flash chromatography (NH_2 capped SiO_2 , 3g, 100% CH_2Cl_2 , 1% MeOH/ CH_2Cl_2) for biological evaluation: TLC R_f = 0.05 (5% MeOH/ CH_2Cl_2); (500 MHz, CDCl_3) δ 8.70–8.56 (m, 2H), 7.65 (d, J = 7.8 Hz, 1H), 7.49 (dd, J = 4.5, 1.5 Hz, 2H), 7.24 (dd, J = 7.8, 1.5 Hz, 1H), 7.10 (d, J = 1.4 Hz, 1H) 5.27 (s, 2H), 5.01 (s, 2H), 4.45 (q, J = 6.9 Hz, 1H), 3.94 (s, 3H), 2.70 (q, J = 7.6 Hz, 2H), 1.55 (d, J = 7.02 Hz, 3H), 1.24 (t, J = 7.6 Hz, 3H); ^{13}C NMR (125 MHz, CDCl_3) δ 173.4, 164.5, 160.8, 156.8, 150.4, 148.4, 138.3, 132.9, 128.5, 121.8, 119.7, 109.3, 101.9, 90.8, 74.8, 55.7, 29.8, 26.9, 22.9, 12.7; IR (neat cm^{-1}) 3446, 3312, 3137, 2928, 2220, 1631, 1571, 1440, 1223, 857; HRMS (DART, M^+ + H) m/z 374.2003 (calculated for $\text{C}_{22}\text{H}_{24}\text{N}_5\text{O}$, 374.1981). HPLC (a) t_R = 5.4 min, 99.1%; (b) t_R = 7.9 min, 99.2%.

4'-[3-(2,4-Diamino-6-ethyl-pyrimidin-5-yl)-1-methyl-prop-2-ynyl]-3'-methoxy-biphenyl-4-ol (30). According to the general Sonogashira coupling procedure, ethyl-iodopyrimidine (0.036 g, 0.14 mmol), CuI (0.0075 g, 0.039 mmol, 21 mol %), $\text{Pd}(\text{PPh}_3)_2\text{Cl}_2$ (0.009 g, 0.014 mmol, 10 mol %), and alkyne **20** (0.037 g, 0.15 mmol) were reacted in DMF/ Et_3N (0.5 mL each) at 60 °C for 14 h. After the mixture was cooled, the dark reddish brown solution was concentrated, and the product was purified by flash chromatography (SiO_2 , 5 g, 3% MeOH/ CH_2Cl_2) to afford coupled pyrimidine **30** as a pale white powder (0.043 g, 79%) followed by reverse phase flash chromatography (NH_2 capped SiO_2 , 3g, 100% CH_2Cl_2 , 1% MeOH/ CH_2Cl_2) for biological evaluation: TLC R_f = 0.06 (5% MeOH/ CH_2Cl_2); mp 188.1–189.3 °C; ^1H NMR (500 MHz, CDCl_3) δ 7.52 (d, J = 7.8 Hz, 1H), 7.42 (d, J = 8.6 Hz, 2H), 7.11 (dd, J = 7.9, 1.7 Hz, 1H), 7.01 (d, J = 1.7 Hz, 1H), 6.90 (d, J = 8.6 Hz, 2H), 5.31 (s, 2H), 4.99 (s, 2H), 4.40 (q, J = 7.0 Hz, 1H), 3.89 (s, 3H), 2.72 (q, J = 7.6 Hz, 2H), 1.53 (d, J = 7.0 Hz, 3H), 1.24 (t, J = 7.6 Hz, 3H); ^{13}C NMR (125 MHz, CDCl_3) δ 173.2, 164.4, 160.3, 156.5, 156.5, 141.4, 133.2, 129.9, 128.6, 128.0, 119.4, 116.1, 109.4, 102.9, 91.4, 73.9, 55.7, 29.7, 26.9, 22.9, 12.9; IR (neat cm^{-1}) 3470, 3371, 3337, 3173, 2970, 2930, 2871, 2341, 1726, 1547, 1438, 1217, 1028, 813; HRMS (ESI, M^+ + H) m/z 389.1963 (calculated for $\text{C}_{23}\text{H}_{25}\text{N}_4\text{O}_2$, 389.1972). HPLC (a) t_R = 6.8 min, 99%; (b) t_R = 8.23 min, 99%.

6-Ethyl-5-[3-(3-methoxy-4'-methyl-biphenyl-4-yl)-but-1-ynyl]-pyrimidine-2,4-diamine (31). According to the general Sonogashira coupling procedure, ethyl-iodopyrimidine (0.026 g, 0.10 mmol), CuI (0.004 g, 0.021 mmol, 21 mol %), $\text{Pd}(\text{PPh}_3)_2\text{Cl}_2$ (0.007 g, 0.010 mmol, 10 mol %), and alkyne **21** (0.031 g, 0.10 mmol) were reacted in DMF/ Et_3N (0.5 mL each) at 60 °C for 14 h. After the mixture was cooled, the dark reddish brown solution was concentrated, and the product was purified by flash chromatography (SiO_2 , 5 g, 2% MeOH/ CHCl_3) to afford coupled pyrimidine **31** as a pale white powder (0.030 g, 77%) followed by reverse phase flash chromatography (NH_2 capped SiO_2 , 3 g, 100% CH_2Cl_2) for biological evaluation: TLC R_f = 0.08 (5% MeOH/ CH_2Cl_2); mp 112.8–114.3 °C; ^1H NMR (500 MHz, CDCl_3) δ 7.57 (d, J = 7.8 Hz, 1H), 7.47 (d, J = 8.1 Hz, 2H), 7.23–7.22 (m, 2H), 7.16 (dd, J = 7.8, 1.6 Hz, 1H), 7.05 (d, J = 1.4 Hz, 1H), 5.13 (s, 2H), 4.79 (s, 2H), 4.42 (q, J = 6.9 Hz, 1H), 3.91 (s, 3H), 2.70 (q, J = 7.6 Hz, 2H), 2.38 (s, 3H), 1.54 (d, J = 7.0 Hz, 3H), 1.24 (t, J = 7.6 Hz, 3H); ^{13}C NMR (125 MHz, CDCl_3) δ 173.4, 164.5, 160.7, 156.5,

141.4, 138.4, 137.3, 130.5, 129.6, 128.1, 127.1, 119.6, 109.6, 102.4, 91.1, 74.5, 55.7, 29.8, 26.9, 23.1, 21.3, 12.7; IR (neat cm^{-1}) 3460, 3387, 3306, 3158, 2969, 2929, 2870, 1727, 1546, 1434, 1221, 805; HRMS (ESI, $\text{M}^+ + \text{H}$) m/z 387.2176 (calculated for $\text{C}_{24}\text{H}_{27}\text{N}_4\text{O}$, 387.2179). HPLC (a) t_R = 36.2 min, 94.8%; (b) t_R = 31.4 min, 96.9%.

4'-[3-(2,4-Diamino-6-ethyl-pyrimidin-5-yl)-1-methyl-prop-2-ynyl]-3'-methoxy-biphenyl-4-carbonitrile (32). According to the general Sonogahisra coupling procedure, ethyl-iodopyrimidine (0.056 g, 0.21 mmol), CuI (0.006 g, 0.031 mmol, 15 mol %), Pd(PPh₃)₂Cl₂ (0.015 g, 0.021 mmol, 10 mol %), and alkyne **22** (0.084 g, 0.318 mmol) were reacted in DMF/Et₃N (1 mL each) at 70 °C for 12 h. After the mixture was cooled, the dark reddish brown solution was concentrated, and the product was purified by flash chromatography (SiO₂, 5 g, 2% MeOH/CHCl₃) followed by reverse phase flash chromatography (NH₂ capped SiO₂, 3 g, 100% CH₂Cl₂, 1% MeOH/CH₂Cl₂) to afford coupled pyrimidine **32** as a pale white powder (0.065 g, 78%); TLC R_f = 0.2 (5% MeOH/CH₂Cl₂); mp 130.9–133.1 °C; ¹H NMR (500 MHz, CDCl₃) δ 7.73–7.70 (m, 2H), 7.69–7.63 (m, 3H), 7.19 (dd, J = 7.8, 1.7 Hz, 1H), 7.05 (d, J = 1.7 Hz, 1H), 5.24 (s, 2H), 4.98 (s, 2H), 4.45 (q, J = 7.0 Hz, 1H), 3.94 (s, 3H), 2.71 (q, J = 7.6 Hz, 2H), 1.55 (d, J = 7.0 Hz, 3H), 1.24 (t, J = 7.6 Hz, 3H); ¹³C NMR (125 MHz, CDCl₃) δ 173.4, 164.5, 160.8, 156.8, 145.7, 139.3, 132.8, 132.5, 128.5, 127.9, 119.9, 119.1, 111.1, 109.6, 101.9, 90.8, 74.8, 55.6, 29.8, 26.9, 23.0, 12.7; IR (neat cm^{-1}) 3464, 3428, 3332, 3188, 3029, 2925, 2775, 2546, 1651, 1548, 1445, 1286, 1008, 735, 557; HRMS (DART, $\text{M}^+ + \text{H}$) m/z 398.1983, (calculated for $\text{C}_{24}\text{H}_{24}\text{N}_5\text{O}$, 398.1981). HPLC (a) t_R = 19.2 min, 99.6%; (b) t_R = 17.5 min, 99.5%.

Carbamic Acid 4'-[3-(2,4-Diamino-6-ethyl-pyrimidin-5-yl)-1-methyl-prop-2-ynyl]-3'-methoxy-biphenyl-4-yl Ester (33). According to the general Sonogahisra coupling procedure, ethyl-iodopyrimidine (0.055 g, 0.21 mmol), CuI (0.008 g, 0.04 mmol, 21 mol %), Pd(PPh₃)₂Cl₂ (0.015 g, 0.021 mmol, 10 mol %), and alkyne **23** (0.092 g, 0.31 mmol) were reacted in DMF/Et₃N (1 mL each) at 60 °C for 12 h. After the mixture was cooled, the dark reddish brown solution was concentrated, and the product was purified by flash chromatography (SiO₂, 5 g, 2% MeOH/CHCl₃) to afford coupled pyrimidine **33** as a pale white powder (0.076 g, 84%) followed by reverse phase flash chromatography (NH₂ capped SiO₂, 3 g, 100% CH₂Cl₂, 1% MeOH/CH₂Cl₂) for biological evaluation: TLC R_f = 0.07 (5% MeOH/CH₂Cl₂); ¹H NMR (500 MHz, MeOD) δ 7.53 (d, J = 7.8 Hz, 1H), 7.46 (d, J = 8.6 Hz, 2H), 7.13 (dd, J = 7.8, 1.60, 1H), 7.11 (d, J = 1.3 Hz, 1H), 6.85 (d, J = 8.6 Hz, 2H), 4.41 (q, J = 6.9 Hz, 1H), 3.93 (s, 3H), 2.67 (q, J = 7.6 Hz, 2H), 1.52 (d, J = 7.0 Hz, 3H), 1.22 (t, J = 7.6 Hz, 3H); ¹³C NMR (125 MHz, MeOD) δ 173.5, 166.1, 162.2, 158.3, 157.9, 142.7, 133.8, 130.9, 129.1, 128.9, 119.9, 116.7, 110.1, 103.2, 91.4, 74.9, 56.2, 30.4, 27.9, 23.4, 13.3; IR (neat cm^{-1}) 3477, 3386, 3336, 3195, 2970, 2929, 2873, 2361, 2023, 1603, 1437, 1217, 1027, 813. HRMS (ESI, $\text{M}^+ + \text{Na}$) m/z 455.1947 (calculated for $\text{C}_{24}\text{H}_{26}\text{N}_5\text{NaO}_3$, 455.1928). HPLC (a) t_R = 6.8 min, 98%; (b) t_R = 8.2 min, 98.7%.

4'-[3-(2,4-Diamino-6-ethyl-pyrimidin-5-yl)-1-methyl-prop-2-ynyl]-3'-methoxy-biphenyl-4-carboxylic Acid Methyl Ester (34). According to the general Sonogahisra coupling procedure, ethyl-iodopyrimidine (0.061g, 0.23 mmol), CuI (0.009 g, 0.05 mmol, 21 mol %), Pd(PPh₃)₂Cl₂ (0.016 g, 0.023 mmol, 10 mol %), and alkyne **24** (0.100 g, 0.34 mmol) were reacted in DMF/Et₃N (1 mL each) at 60 °C for 12 h. After the mixture was cooled, the dark reddish brown solution was concentrated, and the product was purified by flash chromatography (SiO₂, 5g, 2% MeOH/CHCl₃) to afford coupled pyrimidine **34** as a pale white powder (0.077 g, 77%) followed by reverse phase flash chromatography (NH₂ capped SiO₂, 3 g, 100% CH₂Cl₂, 1% MeOH/CH₂Cl₂); TLC R_f = 0.1 (5% MeOH/CH₂Cl₂); mp 168.2–170.8 °C; ¹H NMR (500 MHz, CDCl₃) δ 8.08 (d, J = 8.55 Hz, 2H), 7.64–7.60 (m, 3H), 7.21 (dd, J = 7.8, 1.6 Hz, 1H), 7.08 (d, J = 1.5 Hz, 1H), 5.15 (s, 2H), 4.84 (s, 2H), 4.43 (q, J = 7.0 Hz, 1H), 3.93 (s, 3H), 3.92 (s, 3H), 2.70 (q, J = 7.6 Hz, 2H), 1.54 (d, J = 7.0 Hz, 3H), 1.23 (t, J = 7.6 Hz, 3H); ¹³C NMR (126 MHz, CDCl₃) δ 173.5, 167.2, 164.5, 160.8, 156.7, 145.7, 140.2, 131.9, 130.3, 129.2, 128.3, 127.2, 120.0, 109.7, 102.1, 90.9, 74.7, 55.8, 52.4, 29.9, 26.9, 23.1, 12.8; IR (neat cm^{-1}) 3427, 3302, 3163, 2925, 2851, 2150, 1699, 1548,

1282, 771, 698, 505; HRMS (ESI, $\text{M}^+ + \text{H}$) m/z 431.2081 (calculated for $\text{C}_{25}\text{H}_{27}\text{N}_4\text{O}_3$, 431.2078). HPLC (a) t_R = 20.5 min, 99.4%; (b) t_R = 18.1 min, 99.1%.

5-[3-(4'-Dimethylamino-3-methoxy-biphenyl-4-yl)-but-1-ynyl]-6-ethyl-pyrimidine-2,4-diamine (35). According to the general Sonogahisra coupling procedure, ethyl-iodopyrimidine (0.014 g, 0.05 mmol), CuI (0.002 g, 0.010 mmol, 20 mol %), Pd(PPh₃)₂Cl₂ (0.004 g, 0.005 mmol, 10 mol %), and alkyne (0.015 g, 0.050 mmol) were reacted in DMF/Et₃N (0.5 mL/0.5 mL) at 60 °C for 6 h. After the mixture was cooled, the dark reddish brown solution was concentrated, and the product was purified by flash chromatography (SiO₂, 10g, 100% EtOAc followed by 2% MeOH/CH₂Cl₂) followed by reverse phase flash chromatography (NH₂ capped SiO₂, 5g, 100% CH₂Cl₂) to afford pyrimidine **35** as a off-white solid (9 mg, 43%); TLC R_f = 0.22 (5% MeOH/CH₂Cl₂); mp 135.2–136.1 °C; ¹H NMR (500 MHz, chloroform-*d*) δ 7.51 (d, J = 7.8 Hz, 1H), 7.47 (d, J = 8.6 Hz, 2H), 7.14 (d, J = 5.0 Hz, 1H), 7.03 (s, 1H), 6.78 (d, J = 10.0 Hz, 2H), 5.24 (s, 2H), 5.01 (s, 2H), 4.40 (q, J = 7.0 Hz, 1H), 3.90 (s, 3H), 2.98 (s, 6H), 2.71 (q, J = 7.6 Hz, 2H), 1.53 (d, J = 7.0 Hz, 3H), 1.25 (t, J = 6.9 Hz, 3H); ¹³C NMR (125 MHz, CDCl₃) δ 164.7, 157.9, 156.6, 150.3, 141.9, 129.1, 128.7, 127.9, 119.0, 112.9, 109.2, 103.9, 92.0, 72.3, 55.7, 40.8, 28.1, 26.9, 22.7, 12.6; IR (neat cm^{-1}) 3310, 3172, 2925, 2873, 1603, 1570, 807; HRMS (ES, $\text{M}^+ + \text{H}$) m/z 416.2442 (calculated for $\text{C}_{25}\text{H}_{30}\text{N}_5\text{O}$, 416.2445).

6-Ethyl-5-[3-(4'-fluoro-3-methoxy-biphenyl-4-yl)-but-1-ynyl]-pyrimidine-2,4-diamine (36). According to the general Sonogahisra coupling procedure ethyl-iodopyrimidine (0.10 g, 0.39 mmol), CuI (0.02 g, 0.08 mmol, 20 mol %), Pd(PPh₃)₂Cl₂ (0.03 g, 0.04 mmol, 10 mol %), and alkyne (0.10 g, 0.39 mmol) were reacted in DMF/Et₃N (1 mL/1 mL) at 60 °C for 12 h. After the mixture was cooled, the dark reddish brown solution was concentrated, and the product was purified by flash chromatography (SiO₂, 10 g, 100% EtOAc followed by 1% MeOH/CH₂Cl₂) followed by reverse phase flash chromatography (NH₂ capped SiO₂, 3 g, 100% CH₂Cl₂) to afford pyrimidine **36** as a off-white solid (0.12 g, 79%); TLC R_f = 0.26 (5% MeOH/CH₂Cl₂); mp 129.6–130.0 °C; ¹H NMR (500 MHz, chloroform-*d*) δ 7.56–7.50 (m, 3H), 7.13–7.09 (m, 3H), 7.01 (s, 1H), 5.30 (br s, 2H), 5.19 (br s, 2H) 4.41 (q, J = 6.9 Hz, 1H), 3.91 (s, 3H), 2.73 (q, J = 7.6 Hz, 2H), 1.54 (d, J = 7.0 Hz, 3H), 1.27 (t, J = 7.6 Hz, 3H). ¹³C NMR (125 MHz, CDCl₃) δ 164.5, 162.6 (d, J = 245.0 Hz, 1C), 159.5, 156.6, 140.6, 137.3, 130.5, 128.8 (d, J = 7.5 Hz, 2C), 128.1, 119.7, 115.8 (d, J = 21.2 Hz, 2C), 109.6, 102.8, 91.4, 73.7, 55.7, 29.1, 26.9, 22.9, 12.7; IR (neat cm^{-1}) 3463, 3418, 3309, 3164, 2964, 2927, 1621, 1547, 1432, 1219, 1018; HRMS (DART, $\text{M}^+ + \text{H}$) m/z 391.1921 (calculated for $\text{C}_{23}\text{H}_{24}\text{FN}_4\text{O}$, 391.1934). HPLC (a) t_R = 25.5 min, 96.8%; (b) t_R = 19.8 min, 97.5%.

5-(3-Biphenyl-4-yl-but-1-ynyl)-6-ethyl-pyrimidine-2,4-diamine (37). According to the general Sonogahisra coupling procedure ethyl-iodopyrimidine (0.040 g, 0.15 mmol), CuI (0.006 g, 0.03 mmol, 21 mol %), Pd(PPh₃)₂Cl₂ (0.011 g, 0.02 mmol, 10 mol %), and alkyne **27** (0.034 g, 0.17 mmol) were reacted in DMF/Et₃N (1 mL each) at 60 °C for 12 h. After the mixture was cooled, the dark reddish brown solution was concentrated, and the product was purified by flash chromatography (SiO₂, 5 g, 2% MeOH/CHCl₃) to afford coupled pyrimidine **37** as a pale white powder (0.040 g, 77%) followed by reverse phase flash chromatography (NH₂ capped SiO₂, 3 g, 100% CH₂Cl₂) for biological evaluation: TLC R_f = 0.1 (5% MeOH/CH₂Cl₂); mp 129.3–131.1 °C; ¹H NMR (500 MHz, CDCl₃) δ 7.59–7.55 (m, 4H), 7.48 (d, J = 8. Hz, 2H), 7.42 (dd, J = 7.6, 7.6 Hz, 2H), 7.42 (dd, J = 7.6, 7.6 Hz, 1H), 7.36–7.30 (m, 1H), 5.13 (s, 2H), 4.87 (s, 2H), 4.07 (q, J = 7.1 Hz, 1H), 2.69 (q, J = 7.6 Hz, 2H), 1.61 (d, J = 7.1 Hz, 3H), 1.23 (t, J = 7.6 Hz, 3H); ¹³C NMR (125 MHz, CDCl₃) δ 173.7, 164.5, 160.9, 142.6, 140.9, 140.0, 128.9, 127.6, 127.5, 127.4, 127.3, 101.8, 90.8, 75.6, 32.9, 29.9, 24.9, 12.8; IR (neat cm^{-1}) 3415, 3304, 3162, 2973, 2927, 2871, 1618, 1547, 1436, 1281, 761, 692, 479; HRMS (ESI, $\text{M}^+ + \text{H}$) m/z 343.1907 (calculated for $\text{C}_{22}\text{H}_{23}\text{N}_4$, 343.1917). HPLC (a) t_R = 19.1 min, 98.9%; (b) t_R = 17.3 min, 98.5%.

6-Ethyl-5-[3-(6-phenyl-pyridin-3-yl)-but-1-ynyl]-pyrimidine-2,4-diamine (46). According to the general Sonogahisra coupling procedure, ethyl-iodopyrimidine (0.071 g, 0.27 mmol), CuI (0.011

g, 0.06 mmol, 21 mol %), Pd(PPh₃)₂Cl₂ (0.019 g, 0.03 mmol, 10 mol %), and alkyne **43** (0.061 g, 0.3 mmol) were reacted in DMF/Et₃N (1 mL each) at 60 °C for 12 h. After the mixture was cooled, the dark reddish brown solution was concentrated, and the product was purified by flash chromatography (SiO₂, 5 g, 2% MeOH/CHCl₃) to afford coupled pyrimidine **46** as a pale white hygroscopic solid (0.070 g, 75%), followed by reverse phase flash chromatography (NH₂ capped SiO₂, 3 g, 100% CH₂Cl₂, 1% MeOH/CH₂Cl₂) for biological evaluation: TLC R_f = 0.1 (5% MeOH/CH₂Cl₂); ¹H NMR (500 MHz, CDCl₃) δ 8.72 (d, J = 2.1 Hz, 1H), 7.96 (d, J = 7.2 Hz, 2H), 7.81 (dd, J = 8.2, 2.3 Hz, 1H), 7.70 (d, J = 8.1 Hz, 1H), 7.46 (dd, J = 7.5, 7.5 Hz, 1H), 7.46 (dd, J = 7.5, 7.5 Hz, 1H), 7.41–7.38 (m, 1H), 5.09 (s, 2H), 4.84 (s, 2H), 4.11 (q, J = 7.1 Hz, 1H), 2.68 (q, J = 7.6 Hz, 2H), 1.63 (d, J = 7.1 Hz, 3H), 1.22 (t, J = 7.6 Hz, 3H); ¹³C NMR (125 MHz, CDCl₃) δ 173.9, 164.4, 160.9, 156.4, 148.6, 139.3, 137.3, 135.3, 129.1, 128.9, 127.1, 120.6, 100.6, 90.4, 76.2, 30.6, 29.9, 24.7, 12.7; IR (neat cm⁻¹) 3469, 3308, 3166, 2972, 2931, 1730, 1542, 1435, 1238, 1018, 739, 692; HRMS (ESI, M⁺ + H) m/z 344.1865 (calculated for C₂₁H₂₁N₅, 344.1875). HPLC (a) t_R = 6.9 min, 99.5%; (b) t_R = 7.1 min, 99.2%.

6-Ethyl-5-[3-(6-p-tolyl-pyridin-3-yl)-but-1-ynyl]-pyrimidine-2,4-diamine (47). According to the general Sonogahisra coupling procedure, ethyl-iodopyrimidine (0.059 g, 0.23 mmol), CuI (0.009 g, 0.05 mmol, 21 mol %), Pd(PPh₃)₂Cl₂ (0.016 g, 0.022 mmol, 10 mol %), and alkyne **44** (0.06 g, 0.27 mmol) were reacted in DMF/Et₃N (1 mL each) at 60 °C for 12 h. After the mixture was cooled, the dark reddish brown solution was concentrated, and the product was purified by flash chromatography (SiO₂, 5g, 2% MeOH/CHCl₃) to afford coupled pyrimidine **47** as a pale white powder (0.063 g, 76%) followed by reverse phase flash chromatography (NH₂ capped SiO₂, 3g, 100% CH₂Cl₂, 1% MeOH/CH₂Cl₂) for biological evaluation: TLC R_f = 0.1 (5% MeOH/CH₂Cl₂); mp 144–146.1 °C; ¹H NMR (500 MHz, CDCl₃) δ 8.74 (d, J = 2.2 Hz, 1H), 7.91 (d, J = 8.1 Hz, 2H), 7.82 (dd, J = 8.2, 2.3 Hz, 1H), 7.71 (d, J = 8.2 Hz, 1H), 7.30 (d, J = 8.6 Hz, 2H), 5.25 (s, 2H), 5.07 (s, 2H), 4.13 (q, J = 7.1 Hz, 1H), 2.72 (q, J = 7.6 Hz, 2H), 2.42 (s, 3H), 1.66 (d, J = 7.1 Hz, 3H), 1.26 (t, J = 7.6 Hz, 3H); ¹³C NMR (125 MHz, CDCl₃) δ 173.9, 164.5, 161.1, 156.4, 148.5, 139.1, 136.9, 136.5, 135.2, 129.7, 126.9, 120.3, 100.6, 90.3, 76.2, 30.6, 29.9, 24.6, 21.5, 12.7; IR (neat cm⁻¹) 3459, 3319, 3152, 2973, 2933, 2873, 1542, 1443, 923, 819, 762; HRMS (ESI, M⁺ + H) m/z 358.2013 (calculated for C₂₂H₂₄N₅, 358.2026). HPLC (a) t_R = 9.7 min, 99.7%; (b) t_R = 9.4 min, 99.5%.

6-Ethyl-5-[3-(2-phenyl-pyrimidin-5-yl)-but-1-ynyl]-pyrimidine-2,4-diamine (48). According to the general Sonogahisra coupling procedure, ethyl-iodopyrimidine (0.105 g, 0.4 mmol), CuI (0.028 g, 0.08 mmol, 21 mol %), Pd(PPh₃)₂Cl₂ (0.028 g, 0.04 mmol, 10 mol %), and alkyne **45** (0.123 g, 0.6 mmol) were reacted in DMF/Et₃N (1.3 mL each) at 60 °C for 12 h. After the mixture was cooled, the dark reddish brown solution was concentrated, and the product was purified by flash chromatography (SiO₂, 5 g, 2% MeOH/CHCl₃) to afford coupled pyrimidine **48** as a pale white powder (0.099 g, 71%) followed by reverse phase flash chromatography (NH₂ capped SiO₂, 3g, 100% CH₂Cl₂, 1% MeOH/CH₂Cl₂) for biological evaluation: TLC R_f = 0.1 (5% MeOH/CH₂Cl₂); mp 161.3–162.8 °C; ¹H NMR (500 MHz, CDCl₃) δ 8.84 (s, 2H), 8.62–8.02 (m, 2H), 7.88–7.37 (m, 3H), 5.16 (s, 2H), 4.98 (s, 2H), 4.10 (q, J = 7.1 Hz, 1H), 2.67 (q, J = 7.6 Hz, 2H), 1.65 (d, J = 7.2 Hz, 3H), 1.22 (t, J = 7.6 Hz, 3H); ¹³C NMR (12 MHz, CDCl₃) δ 174.1, 164.4, 163.8, 161.1, 156.1, 137.5, 133.9, 130.9, 128.8, 128.3, 99.2, 89.9, 29.9, 28.7, 24.3, 12.7; IR (neat cm⁻¹) 3401, 3312, 3159, 2970, 2933, 2871, 2222, 1623, 1563, 1427, 802, 740, 687; HRMS (ESI, M⁺ + H) m/z 345.1817 (calculated for C₂₀H₂₁N₆, 345.1822). HPLC (a) t_R = 6.7 min, 99.6%; (b) t_R = 7.6 min, 99.6%.

Crystallization and Structure Determination. *C. glabrata* and *C. albicans* DHFR were expressed and purified as described previously.^{14,32,33} Crystallization of the protein with ligand also followed previously described procedures.³² Briefly, the NADPH and inhibitor (at 1 mM concentration) and protein were incubated for 2 h at 4 °C, concentrated to 17 mg/mL and mixed with reservoir solution (1:1) to form a hanging drop solution. Crystals were harvested and flash frozen. Data were collected at Brookhaven National Laboratory,

beamline X4A (CaDHFR) or X4C (CgDHFR). Molecular replacement was used to determine all three structures using PDB ID 3EEK¹⁵ for CgDHFR and PDB ID 1AOE³⁴ for CaDHFR. Initial phase information was obtained using Phaser;³⁵ electron density and model building were performed with Coot.³⁶ Refinement was carried out with Refmac S³⁷ as part of the CCP4 package. Procheck was used to assess model quality.³⁸

Enzyme Activity. Enzyme inhibition was determined by monitoring the consumption of NADPH at 340 nm for one minute. Reactions were performed with 20 mM TES at pH 7.0, 50 mM KCl, 10 mM 2-mercaptoethanol, 0.5 mM EDTA, and 1 mg/mL bovine serum albumin. Saturating concentrations of cofactor (100 μM NADPH) and substrate (100 μM dihydrofolate) are used with a limiting concentration of enzyme. The enzyme, NADPH, and inhibitor (added as a racemic mixture) are allowed to incubate 5 min before the addition of substrate. Inhibitors are stored as 50 mM stock solutions in DMSO. Stock solutions are diluted in DMSO to appropriate working concentrations so that less than 2% DMSO is added to the assay solution, and inhibition is close to 50%. All assays are conducted in triplicate at 25 °C.

Antifungal Activity. Stock cultures of *C. albicans* (strain SC5314) or *C. glabrata* (strain NCCLS84), thawed from storage in 50% glycerol at –80 °C, were streaked on YM agar plates and grown at 37 °C for 48 h. Isolated colonies from the plate were suspended in 100 mL of glucose–salt–biotin (GSB) media containing ammonia chloride (2 g), potassium phosphate (0.35 g), magnesium sulfate (0.24 g), sodium citrate (0.3 g), piperazine-N,N'-bis[2-ethanesulfonic acid] (3.4 g), biotin (40 mg), and glucose (20 g) in 1 L of water at a final pH of 7.1. Strain SC5314 was grown at 25 °C for 18 h (30 °C for 24–36 h for 5314), and strain NCCLS84 was grown at 37 °C for 48–62 h. An aliquot was removed from the shake flask culture, diluted to between 1 × 10⁵ and 1 × 10⁶ cells/mL in GSB media, and added to 96 well test plates (100 μL per well) containing test compounds dispensed in DMSO (1 μL). Amphotericin B and itraconazole were used as controls.

C. albicans cell viability was determined by the addition of Alamar Blue (10 μL) to each well after a 24 h incubation period. Antifungal activity was determined by observing the shift of maximum absorbance of Alamar Blue 123 from 570 to 600 nm indicating the minimum inhibitory concentration (MIC) of the compound under investigation. NCCLS84 has a much slower rate of metabolism than *C. albicans* strains, and therefore, Alamar blue could not be used to detect cell viability in a reasonable time frame (<24 h). The XTT Cell Proliferation kit (ATCC) was used as an alternative. Tetrazolium dye, XTT, along with an electron-activating reagent (50 μL), is added to 96-well plates and incubated for 24 h at 37 °C. Cell viability is indicated by a color change from a dark orange to a bright orange color that can be detected at 475–550 nm.

Kinetic Solubility Assay. Compounds were initially dissolved as 20 μg/mL dimethyl sulfoxide (DMSO) solutions and diluted in filtered water in the presence or absence of 200 μg/mL methylcellulose (METHOCEL A4M; Dow Corning, Midland, MI). The final concentration of DMSO of all samples is 0.2%. All samples were incubated at room temperature for 30 min and centrifuged for 10 min at 15,000 rpm. The supernatants of the samples were analyzed by reversed phase HPLC. The mobile phase consisted of 50% acetonitrile (ACN) and 50% potassium phosphate buffer (50 mM, pH 7.0), using an isocratic flow rate of 1.5 mL/min. Solubility was determined as the maximal concentration for which absorption is linearly related to the log of the concentration.³⁹

■ ASSOCIATED CONTENT

Supporting Information

Tabular HPLC data, ¹H and ¹³C NMR spectra, statistics for crystallographic data collection and refinement, additional figures, and sequence alignments. This material is available free of charge via the Internet at <http://pubs.acs.org>.

Accession Codes

The Protein Data Bank accession codes are 4HOE, 4HOF, and 4HOG.

AUTHOR INFORMATION

Corresponding Authors

*(D.L.W.) Phone: 860-486-9451. Fax: 860-486-6857. E-mail: dennis.wright@uconn.edu.

*(A.C.A.) Phone: 860-486-6145. Fax: 860-486-6857. E-mail: amy.anderson@uconn.edu.

Author Contributions

[§]N.G.-D. and J.L.P. contributed equally to this work.

Notes

The authors declare no competing financial interest.

ACKNOWLEDGMENTS

We gratefully acknowledge the support of the NIH (GM067542).

ABBREVIATIONS USED

DHFR, dihydrofolate reductase; MIC, minimum inhibitory concentration; BSI, bloodstream infection; IC₅₀, 50% inhibition concentration; CgDHFR, *C. glabrata* DHFR; CaDHFR, *C. albicans* DHFR; NADPH, nicotinamide adenine dinucleotide phosphate; SAR, structure–activity relationship; HPMC, hydroxypropyl methylcellulose; TLC, thin layer chromatography; HRMS, high-resolution mass spectrometry

REFERENCES

- (1) Morrell, M.; Fraser, V.; Kollef, M. Delaying the empiric treatment of *Candida* bloodstream infections until positive blood culture results are obtained: a potential risk factor for hospital mortality. *Antimicrob. Agents Chemother.* **2005**, *49*, 3640–3645.
- (2) Pfaller, M.; Diekema, D. Epidemiology of invasive mycoses in North America. *Crit. Rev. Microbiol.* **2010**, *36*, 1–53.
- (3) Falagas, M.; Roussos, N.; Vardakas, K. Relative frequency of *albicans* and the various non-*albicans* *Candida* spp among candidemia isolates from inpatients in various parts of the world: a systematic review. *Int. J. Infect. Dis.* **2010**, *14*, e954–e966.
- (4) Wisplinghoff, H.; Bischoff, T.; Tallent, S.; Seifert, H.; Wenzel, R.; Edmond, M. Nosocomial bloodstream infections in US hospitals: analysis of 24,179 cases from a prospective nationwide surveillance study. *Clin. Infect. Dis.* **2004**, *39*, 309–317.
- (5) Zilberberg, M.; Schorr, A.; Kollef, M. Secular trends in candidemia-related hospitalization in the United States, 2000–2005. *Infect. Control Hosp. Epidemiol.* **2008**, *29*, 978–980.
- (6) Parkins, M.; Sabuda, D.; Elsayed, S.; Laupland, K. Adequacy of empirical antifungal therapy and effect on outcome among patients with invasive *Candida* species infection. *J. Antimicrob. Chemother.* **2007**, *60*, 613–618.
- (7) Horn, D.; Neofytos, D.; Anaissie, E.; Fishman, J.; Steinback, W.; Olyaei, A.; Marr, K.; Pfaller, M.; Chang, C.; Webster, K. Clinical characteristics of 2,019 patients with candidemia: data from the PATH Alliance Registry. *Clin. Infect. Dis.* **2009**, *48*, 1695–1703.
- (8) Borst, A.; Raimer, M.; Warnock, D.; Morrison, C.; Arthington-Skaggs, B. Rapid acquisition of stable azole resistance by *Candida glabrata* isolates obtained before the clinical introduction of fluconazole. *Antimicrob. Agents Chemother.* **2005**, *49*, 783–787.
- (9) Magill, S.; Shields, C.; Sears, C.; Choti, M.; Merz, W. Triazole cross-resistance among *Candida* spp.: case report, occurrence among bloodstream isolates, and implications for antifungal therapy. *J. Clin. Microbiol.* **2006**, *44*, 529–535.
- (10) Pfaller, M.; Castanheira, M.; Lockhart, S.; Ahlquist, A.; Messer, S.; Jones, R. Frequency of decreased susceptibility and resistance to echinocandins among fluconazole-resistant bloodstream isolates of *Candida glabrata*. *J. Clin. Microbiol.* **2012**, *50*, 1199–1203.
- (11) Kuypers, L.; Bacanari, D.; Jones, M.; Hunter, R.; Tansik, R.; Joyner, S.; Boytos, C.; Rudolph, S.; Knick, V.; Wilson, H. R.; Caddell, J. M.; Friedman, H.; Comley, J.; Stables, J. High-affinity inhibitors of dihydrofolate reductase: antimicrobial and anticancer activities of 7,8-dialkyl-1,3-diaminopyrrolo[3,2-*f*]quinazolines with small molecular size. *J. Med. Chem.* **1996**, *39*, 892–903.
- (12) Otzen, T.; Wempe, E.; Kunz, B.; Bartels, R.; Lehwark-Yvetot, G.; Hansel, W.; Schaper, K.; Seydel, J. Folate-synthesizing enzyme system as target for development of inhibitors and inhibitors combinations against *Candida albicans*: Synthesis and biological activity of new 2,4-diaminopyrimidines and 4'-substituted 4-amino-diphenyl sulfones. *J. Med. Chem.* **2004**, *47*, 240–253.
- (13) Ziegelbauer, K. A dual labelling method for measuring uptake of low molecular weight compounds into the pathogenic yeast *Candida albicans*. *Med. Mycol.* **1998**, *36*, 323–330.
- (14) Liu, J.; Bolstad, D.; Smith, A.; Priestley, N.; Wright, D.; Anderson, A. Structure-guided development of efficacious antifungal agents targeting *Candida glabrata* dihydrofolate reductase. *Chem. Biol.* **2008**, *15*, 990–996.
- (15) Liu, J.; Bolstad, D.; Smith, A.; Priestley, N.; Wright, D.; Anderson, A. Probing the active site of *Candida glabrata* dihydrofolate reductase with high resolution crystal structures and the synthesis of new inhibitors. *Chem. Biol. Drug Des.* **2009**, *73*, 62–74.
- (16) Paulsen, J.; Viswanathan, K.; Wright, D.; Anderson, A. Structural analysis of the active sites of dihydrofolate reductase from two species of *Candida* uncovers ligand-induced conformational changes shared among species. *Bioorg. Med. Chem. Lett.* **2013**, *23*, 1279–1284.
- (17) Ziegelbauer, K.; Grusdat, G.; Schade, A.; Paffhausen, W. High throughput assay to detect compounds that enhance the proton permeability of *Candida albicans* membranes. *Biosci. Biotechnol. Biochem.* **1999**, *63*, 1246–1252.
- (18) Klis, F.; Sosinska, G.; DeGroot, P.; Brul, S. Covalently linked cell wall proteins of *Candida albicans* and their role in fitness and virulence. *FEMS Yeast Res.* **2009**, *9*, 1013–1028.
- (19) deNobel, J.; Klis, F.; Priem, J.; Munnik, T.; van den Ende, H. The glucanase-soluble mannoproteins limit cell wall porosity in *Saccharomyces cerevisiae*. *Yeast* **1990**, *6*, 491–499.
- (20) Yin, Q.; deGroot, P.; deKoster, C.; Klis, F. Mass spectrometry-based proteomics of fungal wall glycoproteins. *Trends Microbiol.* **2008**, *16*, 20–26.
- (21) Zlotnick, H.; Fernandez, M.; Bowers, B.; Cabib, E. *Saccharomyces cerevisiae* mannoproteins form an external cell wall layer that determines wall porosity. *J. Bacteriol.* **1984**, *159*, 1018–1026.
- (22) Fradin, C.; Slomianny, M.; Mille, C.; Masset, A.; Robert, R.; Sendid, B.; Ernst, J.; Michalski, J.; Poulain, D. Beta-1,2 oligomannose adhesin epitopes are widely distributed over the different families of *Candida albicans* cell wall mannoproteins and are associated through both N- and O-glycosylation processes. *Infect. Immun.* **2008**, *76*, 4509–4517.
- (23) Horisberger, M.; Clerc, M. Ultrastructural localization of anionic sites on the surface of yeast, hyphal and germ-tube forming cells of *Candida albicans*. *Eur. J. Cell Biol.* **1988**, *46*, 444–452.
- (24) Weig, M.; Jansch, L.; Gross, U.; DeKoster, C.; Klis, F.; deGroot, P. Systematic identification in silico of covalently bound cell wall proteins and analysis of protein-polysaccharide linkages of the human pathogen *Candida glabrata*. *Microbiology* **2004**, *150*, 3129–3144.
- (25) Beierlein, J.; Karri, N.; Anderson, A. Targeted mutations of *Bacillus anthracis* dihydrofolate reductase condense complex structure-activity relationships. *J. Med. Chem.* **2010**, *53*, 7327–7336.
- (26) Bolstad, D.; Bolstad, E.; Frey, K.; Wright, D.; Anderson, A. A structure-based approach to the development of potent and selective inhibitors of dihydrofolate reductase from *Cryptosporidium*. *J. Med. Chem.* **2008**, *51*, 6839–6852.
- (27) Viswanathan, K.; Frey, K.; Scocchera, E.; Martin, B.; Swain, P.; Alverson, J.; Priestley, N.; Anderson, A.; Wright, D. Toward new therapeutics for skin and soft tissue infections: Propargyl-linked

antifolates are potent inhibitors of MRSA and *Streptococcus pyogenes*. *PLoS One* **2012**, 7 (2), e29434.

(28) Wurtz, N.; Priestley, E.; Cheney, D.; Glunz, P.; Zhang, X.; Ladziata, V.; Parkhurst, B.; Mueller, L. Macrocyclic Factor VIIA Inhibitors Useful as Anticoagulants. WO2008079836, July 3, 2008.

(29) Matulenko, M.; Lee, C.-H.; Jiang, M.; Frey, R.; Cowart, M.; Bayburt, E.; DiDomenico, J.; Gfesser, G.; Gomtsyan, A.; Zheng, G.; McKie, J.; Stewart, A.; Yu, H.; Kohlhaas, L.; Alexander, K.; McGaraughty, S.; Wismer, C.; Mikusa, J.; Marsh, K.; Snyder, R.; Diehl, M.; Kowaluk, E.; Jarvis, M.; Bhagwat, S. 5-(3-bromophenyl)-7-(6-morpholin-4-ylpyridin-3-yl)pyrido-[2,3-d]pyrimidin-ylamine: Structure–activity relationships of 7-substituted heteroaryl analogs as non-nucleoside adenosine kinase inhibitors. *Bioorg. Med. Chem.* **2005**, 13, 3705.

(30) Pietruszka, J.; Witt, A. Synthesis of the Bestmann–Ohira reagent. *Synthesis* **2006**, 4266–4268.

(31) Richardson, M. L.; Stevens, M. F. G. Structural studies on bioactive compounds. Part 37. Suzuki coupling of diaminopyrimidines: a new synthesis of the antimalarial drug pyrimethamine. *J. Chem. Res. Synopses* **2002**, 10, 482.

(32) Paulsen, J.; Bendel, S.; Anderson, A. Crystal structures of *Candida albicans* dihydrofolate reductase bound to propargyl-linked antifolates reveal the flexibility of active site residues critical for ligand potency and selectivity. *Chem. Biol. Drug Des.* **2011**, 78, 505–512.

(33) Paulsen, J.; Liu, J.; Bolstad, D.; Smith, A.; Priestley, N.; Wright, D.; Anderson, A. In vitro biological activity and structural analysis of 2,4-diamino-5-(2'-arylpropargyl)pyrimidine inhibitors of *Candida albicans*. *Bioorg. Med. Chem.* **2009**, 17, 4866–4872.

(34) Whitlow, M.; Howard, A.; Stewart, D.; Hardman, K.; Kuyper, L.; Baccanari, D.; Fling, M.; Tansik, R. X-ray crystallographic studies of *Candida albicans* dihydrofolate reductase. *J. Biol. Chem.* **1997**, 272, 30289–30298.

(35) McCoy, A. Solving structures of protein complexes by molecular replacement with Phaser. *Acta Crystallogr., Sect. D* **2007**, 63, 32–41.

(36) Emsley, P.; Cowtan, K. Coot: Model-building tools for molecular graphics. *Acta Crystallogr., Sect. D* **2004**, 60, 2126–2132.

(37) Murshudov, G.; Vagin, A.; Dodson, E. Refinement of macromolecular structures by the maximum-likelihood method. *Acta Crystallogr., Sect. D* **1997**, 53, 240–255.

(38) Laskowski, R.; MacArthur, M.; Moss, D.; Thornton, J. PROCHECK: a program to check the stereochemical quality of protein structures. *J. Appl. Crystallogr.* **1993**, 26, 283–291.

(39) Zhou, W.; Viswanathan, K.; Hill, D.; Anderson, A.; Wright, D. Acetylenic linkers in lead compounds: A study of the stability of the propargyl-linked antifolates. *Drug Metab. Dispos.* **2012**, 40, 2002–2008.